Table 2 Pharmacodynamic parameters[a] of quazepam following the administration of a single oral administration with grape fruit juice (GFJ) or water

	DSST (digits/h)		Drowsiness (VAS mm/h)		Mental slowness (VAS mm/h)	
	AUC(0–6)	AUC(0–12)	AUC(0–6)	AUC(0–12)	AUC(0–6)	AUC(0–12)
Triazolam + water	−49 (−68, −26)	−57 (−100, −15)	160 (42, 277)	200 (−13, 412)	126 (59, 192)	212 (64, 360)
Triazolam + GFJ	−64 (−98, −31)	−58 (−102, −14)	147 (33, 261)	136 (−88, 360)	126 (55, 198)	146 (−12, 305)
Quazepam + water	−9 (−30, 12)a,b[b]	0 (−40, 39)	187 (81, 292)	343 (116, 569)	100 (25, 175)	191 (19, 363)
Quazepam + GFJ	−6 (−22, 11)a,b	5 (−28, 37)a,b	162 (114, 210)	283 (196, 370)	88 (33, 143)	188 (85, 292)

[a]DSST, Digit substitution symbol test; VAS, visual analog scale; AUC(0-*n*), area under the symbol number or analog scale-time curve between time zero and *n* hours after administration

[b]Data are mean values (90% confidence interval); values followed by 'a', $p<0.05$ versus triazolam + water; values followed by 'b', $p<0.05$ versus triazolam + GFJ

reach statistical significance. The concentration of *N*-desmethyl-2-oxoquazepam in the plasma rose up to 24 h following the administration of quazepam; consequently, the C_{max} of this metabolite could not be determined in this study. However, GFJ did not affect the plasma concentrations of this metabolite during the period we examined (Fig. 3b). No significant difference in the GFJ-related increase in AUC(0–24) was observed between triazolam and quazepam (difference: 58%). There was also no significant difference in the increase in C_{max} between triazolam (+55%) and quazepam (+62%). The increase in the AUC(0–24) or C_{max} of 2-oxoquazepam did not significantly differ from that of triazolam. The ratio of 2-oxoquazepam to quazepam in the C_{max} or AUC(0–24) did not differ between two trials C_{max}: water, 0.21; C_{max}: GFJ, 0.19; AUC(0–24): water, 0.24; AUC(0–24): GFJ, 0.22). The $t_{½}$ (in hours) of these agents did not significantly differ between the water and GFJ trials (quazepam: water, 5.9; quazepam: GFJ, 4.5; 2-oxoquazepam: water, 6.3; 2-oxoquazepam: GFJ, 5.8).

Pharmacodynamics

Triazolam remarkably reduced the number of digit substitutions (Fig. 4, Table 2). On the other hand, the effect of quazepam on the objective performance in the DSST was small. Triazolam with GFJ caused an addition decrease in digit substitution, especially at 2 h following administration of the dose (Fig. 4). However, GFJ did not deteriorate the performance in the DSST after the quazepam dose.

Triazolam caused significant ($p<0.0001$) drowsiness and mental slowness, with a peak at 2 h after administration of the dose (Fig. 5). Time courses of other subjective effects were similar (data not shown). Quazepam also produced similar sedative-like drug effects but its peak was slightly later – at 4–6 h after administration of the dose (Fig. 5). GFJ did not significantly enhance these triazolam- or quazepam-induced subjective effects (Table 2).

A significant negative correlation was noted between triazolam concentrations in the plasma and the decrease in

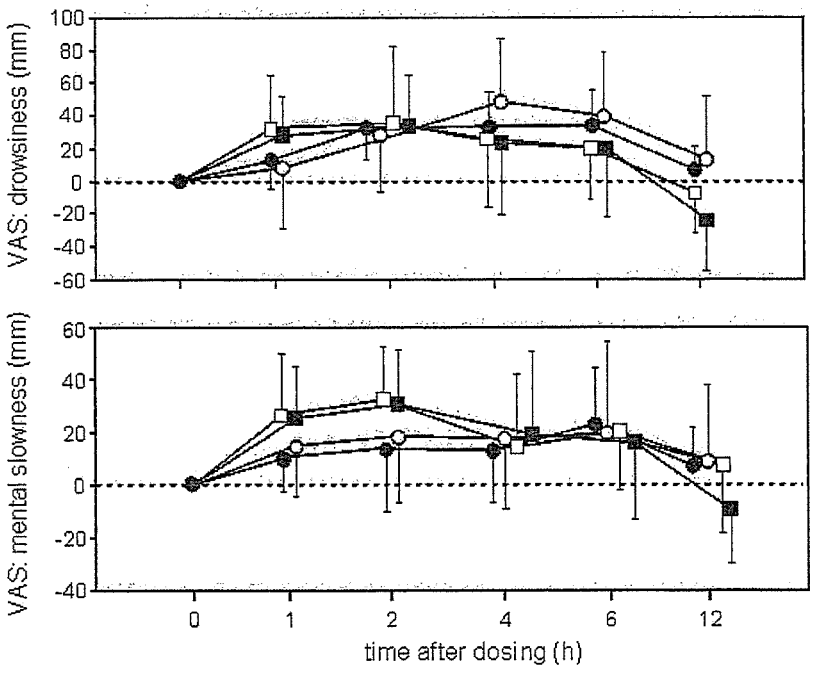

Fig. 5 Sedative-like self-rated drug effects [based on scores from the 100-mm visual analog scale (VAS), expressed as changes over the predose baseline] after a single oral dose of 0.25 mg triazolam or 15 mg quazepam with grapefruit juice or water. *Open circle* Quazepam with water, *black circle* quazepam with grapefruit juice, *open square* triazolam with water, *black square* triazolam with grapefruit juice. Points represent the mean (n=9) ± SD

the number of digit substitutions at 2 h after the dose had been given (R=−0.539, p<0.05, n=18). There were no significant correlations between the plasma concentrations of quazepam or 2-oxoquazepam and any pharmacodynamic parameters.

Discussion

In this study, the C_{max} of triazolam, quazepam and 2-oxoquazepam significantly increased during the trials with GFJ. The oral bioavailability of triazolam was about 60% due to presystemic elimination. Triazolam is mainly metabolized by CYP3A4 [8], and the elimination $t_{½}$ is 2–4 h. The bioavailability of quazepam is assumed to be 29–35% based on a calculation of the ratio of the dose-normalized cumulative amount excreted in Japanese subjects (personal communication, Mitsubishi Pharma, Tokyo, Japan). Quazepam is metabolized by CYP3A4 and CYP2C9 [11], and it has been reported that in plasma the elimination $t_{½}$ of quazepam and an active metabolite, 2-oxoquazepam, are 25–40 h and that of *N*-desmethyl-2-oxoquazepam is 70–75 h [14, 15]. The calculated elimination $t_{½}$ of quazepam and 2-oxoquazepam in the present study were shorter than those reported in the previous studies because the length of sampling period was not enough to estimate terminal half-lives of these compounds. In the present study, the effect of GFJ on the pharmacokinetics of quazepam and its metabolites were examined for 24 hours after administration of the dose; however, a longer sampling period post-dose administration and an analysis system with a high sensitivity are required to correctly estimate the half-lives of quazepam, 2-oxoquazepam and in particular *N*-desmethyl-2-oxoquazepam. In fact, we were unable to determine even the C_{max} for *N*-desmethyl-2-oxoquazepam.

The metabolism of quazepam and 2-oxoquazepam is mediated by CYP3A4 and CYP2C9, and the contribution of CYPs to the metabolic process is presumed to be 50:50 based on an inhibition study using the cDNA-expressed human CYPs and antiserum for CYP3A4 and CYP2C [11]. These findings led us to speculate that the inhibition of CYP3A4 activity by GFJ has a greater influence on the pharmacokinetics of triazolam than on those of quazepam. The AUC(0–24) of triazolam was significantly increased by GFJ, while the elevation in this parameter for quazepam or 2-oxoquazepam by GFJ did not reach statistical significance. However, the GFJ-related changes of AUC (0–24) or C_{max} for triazolam did not significantly differ from those for quazepam or 2-oxoquazepam. It therefore appears that the inhibition of intestinal CYP3A4 activities by GFJ enhances the oral bioavailability of both quazepam and triazolam. The ratio of 2-oxoquazepam to quazepam in the C_{max} or AUC(0–24) did not differ significantly between the trials with and without GFJ. GFJ elevated the plasma concentrations of quazepam and 2-oxoquazepam, but not of *N*-desmethyl-2-oxoquazepam. The quazepam metabolite 2-oxoquazepam is further metabolized to *N*-desmethyl-2-oxoquazepam by CYP3A4 and CYP2C9 and to another metabolite by CYP3A4 [11]. Consequently, it is likely that in the present study the effect of GFJ diminished with the formation of *N*-desmethyl-2-oxoquazepam. In addition, GFJ did not prolong the $t_{½}$ of triazolam, quazepam and 2-oxoquazepam. These pharmacokinetic alterations may be caused by the GFJ-induced inhibition of CYP3A4 activity in the intestine, but not in the liver [5]. Lilja et al. [10] been reported that repeated consumption of GFJ prolonged the $t_{½}$ of triazolam, suggesting the inhibition of hepatic CYP3A4 by GFJ. In their study, subjects were given 200 ml of double-strength GFJ three times a day for 3 days, while we gave 250 ml of normal-strength GFJ three times a day for 4 days to our participants. Not only the length of the treatment period but the strength of GFJ may be a determinant of the GFJ-induced inhibition of hepatic CYP3A4, if this inhibition is truly caused by GFJ.

GFJ increases plasma triazolam concentration [9, 10], which is consistent with the present results. A significant increase in the pharmacodynamic effects of triazolam has been observed following multiple doses of GFJ [10], but not following a single dose [9, 16]. Hukkinen et al. [9] found that psychomotor function, as assessed by DSST, was not further impaired by a single dose of 250 ml GFJ despite an increase in plasma triazolam concentration [9]. In their study, triazolam C_{max} increased by only 30% following a single dose of GFJ. Similarly, Vanakoski et al. [16] observed that a single, concomitant ingestion of 300 ml GFJ did not influence the triazolam-induced objective effects, including DSST. In the present study in which multiple-doses of GFJ were given, C_{max} increased by 55% on average; furthermore, the maximum reduction in DSST performance showed a weak – but significant – correlation with the plasma concentration of triazolam. The present results suggest that pharmacodynamic alteration by the GFJ-triazolam interaction may be caused by the increase in plasma triazolam concentration. Taken together, a single dose of GFJ may not enough to cause the interaction with triazolam on psychomotor function, probably because of an insufficient increase in plasma triazolam concentration.

GFJ increased plasma quazepam and 2-oxoquazepam concentrations, but it did not alter the pharmacodynamic effects. The major metabolites of quazepam, 2-oxoquazepam and *N*-desmethyl-2-oxoquazepam are reported to be pharmacologically active, although the involvement of these metabolites has not been proven to date. Roth et al. [17] suggested that the hypnotic effect of quazepam is caused by the metabolite *N*-desmethyl-2-oxoquazepam [17]. In their study, a repeated dose of quazepam, however, did not increase the incidence or the duration of daytime napping; similarly, the hypnotic and sedative effect of quazepam disappeared 12 h after the dose despite a high plasma concentration of *N*-desmethyl-2-oxoquazepam. If the effect of quazepam is solely caused by *N*-desmethyl-2-oxoquazepam, the sedative-like subject-rated effects quazepam should have been evident even 12 h after administration of the dose of quazepam. However, we observed the maximum sedative-like subject-rated effects by quazepam 4–6 h after the dose. It therefore appears that the sedative effect observed in the present study was caused

by quazepam itself. A contribution by 2-oxoquazepam to the effects of quazepam is possible, but it is not obvious based on our results, and the contribution of *N*-desmethyl-2-oxoquazepam was small, if any. The effect of quazepam on psychomotor function as assessed by DSST was negligible, a result similar to that found by Nikaido et al. [18]. Our results suggest that the detrimental effects of 15 mg quazepam on psychomotor functions may be small even if the drug is taken with GFJ. However, 0.25 mg triazolam and 15 mg quazepam produced significant sedative-like, subject-rated effects in this study. The effect of GFJ on plasma quazepam or 2-oxoquazepam concentration was diminished at 4–6 h after the dose had been given, which is the time span when the sedative effect was at its maximum; consequently, the subject-rated effect of quazepam may not be enhanced by GFJ.

CYP2C9 metabolizes many clinically important drugs including the S-enantiomer of warfarin and tolbutamide [19]. The enzyme is also involved in the metabolism of quazepam [11]. Two common polymorphisms of CYP2C9 have been reported; the *2 allele (Arg144Cys) and the *3 allele (Ile359Leu) [20]. CYP2C9*2 and CYP2C9*3 diminish the clearance of S-warfarin and tolbutamide, respectively [19]. The frequencies of these alleles are as follows: CYP2C9*2, 8% in Caucasians and 0% in Japanese; CYP2C9*3: 6% in Caucasians and 2% in Japanese [12, 21]. Therefore, when quazepam is given to patients with one or these CYP2C9 polymorphisms, the effects of GFJ on the pharmacokinetics and pharmacodynamics of the drug may be exaggerated. Further study is needed to address the issue.

In summary, the results of this study demonstrate that the effects of GFJ on the pharmacodynamics of triazolam are greater than on those of quazepam. These GFJ-induced different effects are partly explained by the fact that triazolam is mainly metabolized by CYP3A4 while quazepam is metabolized by CYP3A4 and CYP2C9.

Acknowledgements We thank Ms. Junko Koyano, Hiroko Susuki and Mariko Hojo for their technical assistance.

References

1. Edgar B, Bailey D, Bergstrand R, Johnsson G, Regardh CG (1992) Acute effects of drinking grapefruit juice on the pharmacokinetics and dynamics of felodipine and its potential clinical relevance. Eur J Clin Pharmacol 42:313–317
2. Benton RE, Honig PK, Zamani K, Cantilena LR, Woosley RL (1996) Grapefruit juice alters terfenadine pharmacokinetics, resulting in prolongation of repolarization on the electrocardiogram. Clin Pharmacol Ther 59:383–388
3. Ducharme MP, Warbasse LH, Edwards DJ (1995) Disposition of intravenous and oral cyclosporine after administration with grapefruit juice. Clin Pharmacol Ther 57:485–491
4. Lilja JJ, Kivistö KT, Neuvonen PJ (1998) Grapefruit juice-simvastatin interaction: Effect on serum concentrations of simvastatin, simvastatin acid, and HMG-CoA reductase inhibitors. Clin Pharmacol Ther 64:477–483
5. Lown KS, Bailey DG, Fontana RJ, Janardan JK, Adair CH, Fortlage LA, Brown MB, Guo W, Watkins PB (1997) Grapefruit juice increases felodipine oral bioavailability in human by decreasing intestinal CYP3A protein expression. J Clin Invest 99:2545–2553
6. Fukuda K, Ohta T, Oshima Y, Ohashi N, Yoshikawa M, Yamazoe Y (1997) Specific CYP3A4 inhibitors in grapefruit juice: furanocoumarin dimers as components of drug inhibition. Pharmacogenetics 7:391–396
7. Paine MF, Criss AB, Watkins PB (2004) Two major grapefruit juice components differ in intestinal CYP3A4 inhibition kinetics and binding properties. Drug Metab Dispos 32:1146–1153
8. Moltke LL von, Greenblatt DJ, Harmatz JS, Duan SX, Harrel JM, Catreau-Bibbo NM, Pritchard GA, Wright CE, Shader RI (1996) Triazolam biotransformation by human liver microsomes in vitro: effects of metabolic inhibitors and clinical confirmation of a predicted interaction with ketoconazole. J Pharmacol Exp Ther 276:370–379
9. Hukkinen SK, Varhe A, Olkkola KT, Neuvonen PJ (1995) Plasma concentrations of triazolam are increased by concomitant ingestion of grapefruit juice. Clin Pharmacol Ther 58:127–131
10. Lilja JJ, Kivistö KT, Backman JT, Neuvonen PJ (2000) Effect of grapefruit juice dose on grapefruit juice-triazolam interaction: repeated consumption prolongs triazolam half-life. Eur J Clin Pharmacol 56:411–415
11. Fujisaki H, Hirotsu K, Ogawa T, Mizuki K, Mizuta H, Arima N (2001) Metabolism of quazepam and its metabolites in humans: Identification of metabolic enzymes and evaluation of drug interaction in vitro (in Japanese with English abstract). Yakubutsudoutai (Xenobio Metabol Dispos) 16:558–568
12. Nasu K, Kubota T, Ishizaki T (1997) Genetic analysis of CYP2C9 polymorphism in a Japanese population. Pharmacogenetics 7:405–409
13. Sostmann HJ, Sostmann H, Crevoisier C, Bircher J (1989) Dose equivalence of midazolam and triazolam: A psychometric study based on flicker sensitivity, reaction time and digit symbol substitution test. Eur J Clin Pharmacol 36:181–187
14. Chung M, Hilbert JM, Gural RP, Radwaniski E, Symchowicz S, Zampaglinone N (1984) Multiple-dose quazepam kinetics. Clin Pharmacol Ther 35:520–524
15. Hilbert JM, Chung M, Maier G, Grural R, Symchowicz S, Zampaglinone N (1984) Effect of sleep on quazepam kinetics. Clin Pharmacol Ther 36:99–104
16. Vanakoski J, Mattila MJ, Seppälä T (1996) Grapefruit juice does not enhance the effects of midazolam and triazolam in man. Eur J Clin Pharmacol 50:501–508
17. Roth TG, Roehrs TA, Koshorek GL, Greenblatt DJ, Rosenthal LD (1997) Hypnotic effects of low doses of quazepam in older insomniacs. J Clin Psychopharmacol 17:401–406
18. Nikaido AM, Ellinwood EH Jr (1987) Comparison of the effects of quazepam and triazolam on cognitive-neuromotor performance. Psychopharmacology 92:459–464
19. Goldstein JA, de Morais SM (1994) Biochemistry and molecular biology of the human CYP2C subfamily. Pharmacogenetics 4:285–299
20. Goldstein JA (2001) Clinical relevance of genetic polymorphisms in the human CYP2C subfamily. Br J Clin Pharmacol 52:349–355
21. Sullivan-Klose TH, Ghanayem BI, Bell DA, Zhang ZY, Kaminsky LS, Shenfield GM, Miners JO, Birkett DJ, Goldstein JA (1996) The role of the CYP2C9-Leu359 allelic variant in the tolbutamide polymorphism. Pharmacogenetics 6:341–349

http://www.kidney-international.org

Indoxyl sulfate stimulates proliferation of rat vascular smooth muscle cells

H Yamamoto[1,2], S Tsuruoka[1,2], T Ioka[1], H Ando[2], C Ito[1], T Akimoto[1], A Fujimura[2], Y Asano[1] and E Kusano[1]

[1]*Department of Nephrology, Jichi Medical School, Tochigi, Japan and* [2]*Department of Clinical Pharmacology, Jichi Medical School, Tochigi, Japan*

Vascular smooth muscle cell (VSMC) proliferation is a key event in the progression of arteriosclerosis. Clinical studies show that uremic toxins deteriorate the arteriosclerosis in renal failure patients. Indoxyl sulfate (IS) is a strong protein-bound uremic toxin, but the effect of IS on VSMC proliferation has not been studied. We examined the effect of IS on rat VSMC proliferation, assessed by a cell counting kit (4-[3-[4-Iodophenyl]-2-4(4-nitrophenyl)-2*H*-5-tetrazolio-1, 3-benzene disulfonate] assay) and by [^{3}H]thymidine incorporation *in vitro*. We further evaluated a contribution of mitogen-activated protein kinase (MAPK; p44/42 MAPK) to VSMC proliferation by IS. Immunohistochemical staining was performed for VSMCs using antirat organic anion transporter (OAT)3 antibody. The mRNA expressions of platelet-derived growth factor (PDGF)-A and -C chains, and PDGF-β receptor were evaluated by real-time PCR. IS stimulated the proliferation of VSMCs in a concentration-dependent manner and activated p44/42 MAPK. Concentration of IS needed to stimulate the proliferation of rat VSMC was about 250 μM, which is compatible with that in the serum of end-stage renal failure patients. PD98059 (10 μM), a selective inhibitor of MAPK/extracellular signal-regulated kinase, inhibited the IS-induced (250 μM) VSMC proliferation and phosphorylation of MAPK. Probenecid (0.5 mM), an inhibitor and substrate of OAT, inhibited the IS-induced (250 μM) VSMC proliferation. Rat OAT3 was detected in VSMCs. The mRNA expressions of PDGF-C chain and PDGF-β receptor were significantly increased by IS. We conclude that IS directly stimulates rat VSMC proliferation and activates MAPK *in vitro*. This might be one of the mechanisms underlying the progression of atherosclerotic lesions in end-stage renal disease patients.

Kidney International (2006) **69,** 1780–1785. doi:10.1038/sj.ki.5000340; published online 12 April 2006

KEYWORDS: indoxyl sulfate; uremic toxin; vascular smooth muscle cells; MAP kinase cascade; organic anion transporter

Correspondence: *S Tsuruoka, Department of Pharmacology, Division of Clinical pharmacology, Jichi Medical School, 3311 Yakushiji, Minamikawachi, Kawachi, Tochigi 329-0498, Japan. E-mail: tsuru@jichi.ac.jp*

Received 4 April 2005; revised 5 November 2005; accepted 14 December 2005; published online 12 April 2006

Improvements in dialysis treatment have resulted in prolongation of the survival period of hemodialysis patients, but their prognosis is still poor compared to that in the general population.[1] The major cause of death in patients undergoing dialysis is cardiovascular disease.[2] The pathophysiology of cardiovascular disease in end-stage renal disease patients is not completely understood; however, accumulation of uremic toxins that are difficult to be removed from the body by current dialysis procedures is partly involved in the condition.[3,4] Indoxyl sulfate (IS) is one of the organic anions metabolized in the liver from indole, which is produced by the intestinal bacteria as a metabolite of tryptophan.[5] Although the molecular weight of IS is small, the rate of binding to albumin is high in the blood,[6] which, in turn, leads to its large secretion from the proximal tubule cells in urine.[7] Various organic anion transporters (OATs) exist in proximal tubules, and it has recently been revealed that IS is secreted in urine mainly by OAT3, one of the members of the OAT family.[8] Therefore, IS accumulates in the body of patients with reduced renal function.[5]

Removal of IS by hemodialysis is difficult because the size of the IS–albumin complex molecule in blood is larger than the pore size of a dialysis membrane.[5] Thus, IS is considered to be one of the main uremic toxins that are difficult to be removed from the body by current dialysis procedures.[5] It has been reported that IS accelerates the progression of renal failure,[9] but only one datum is available about the effects of IS on the cardiovascular system.[10]

In the progression of atherosclerotic lesions, the proliferation of vascular smooth muscle cells (VSMCs) is of particular importance. The mitogen-activated protein kinase (MAPK) cascades are a well-documented family of serine/threonine kinases that include p44/42 MAPK (also called extracellular signal-regulated kinases (ERK1/2)), p38 MAPK, and c-Jun N-terminal kinase.[11] The p44/42 MAPK cascade is the most well characterized and is shown to mediate proliferative responses in various cells, including mesangial cells[12] and VSMCs.[13] Growth factors, such as platelet-derived growth factor (PDGF),[14] angiotensin II,[15] erythropoietin,[16] and uremic toxins such as homocysteine,[17] and uric acid[18] can activate intracellular signaling cascades, leading to the proliferation of VSMCs. However, the effects of IS on VSMC proliferation and activation of MAPK have not been studied.

In this study, we therefore directly investigated the effects of IS *in vitro* on VSMC proliferation and MAPK activation using cultured rat VSMCs.

RESULTS

IS increases rat VSMC proliferation and DNA synthesis

First, we examined the effect of IS on the number of VSMCs. IS significantly increased the number of VSMCs in a concentration-dependent manner (Figure 1). PDGF (10 ng/ml) also increased the number of VSMCs.

We next evaluated whether the increase in cell proliferation was accompanied with DNA synthesis. Figure 2a shows that [^{3}H]thymidine incorporation was also significantly increased by IS (100–500 μM). Because IS is mainly bound to albumin in the serum, we also evaluated the effect of IS in the presence of 4 g/dl albumin in the medium. Although basal value was significantly lower with albumin, IS at 250 and 500 μM significantly increased the uptake (Figure 2b). This result indicates that IS stimulated VSMC proliferation even in the presence of 4 g/dl albumin. IS in the body is made from tryptophan in the intestine[5] and the medium used in this study contained tryptophan (78 μM), which may affect the results. Thus, we further examined the effect of the removal of tryptophan from the medium. As shown in Figure 3, 250 μM IS increased the [^{3}H]thymidine incorporation by VSMCs in both the presence and absence of tryptophan (78 μM). Therefore, IS, but not its precursor, directly stimulated the proliferation of VSMC *in vitro*.

As IS is reported to be the substrate of OAT3 in the proximal tubule cell membrane,[8] we next examined whether the proliferation of VSMCs is mediated by cellular transport of IS via the OAT. As shown in Figure 4, the increase of [^{3}H]thymidine incorporation in VSMCs by 250 μM IS was partly prevented by co-administration of 0.5 mM probenecid, an inhibitor and substrate of OAT,[8] whereas probenecid alone did not affect it. Next, to determine whether OAT3 is present in rat VSMCs, we performed immunostaining of rat VSMCs by rat OAT3 antibody. As shown in Figure 5, the rat VSMCs had strong signals of rat OAT3, mainly in the cell membrane.

IS activates the p44/42MAPK pathway in rat VSMCs

To evaluate further intracellular signaling event in the effects of IS on the rat VSMC proliferation, we investigated the

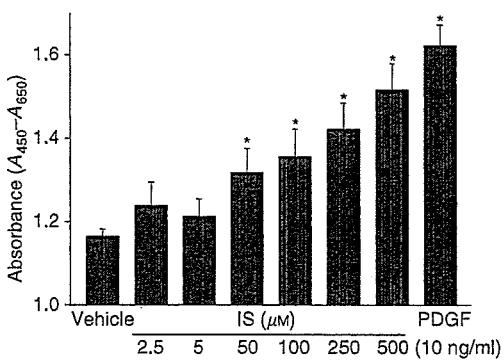

Figure 1 | Effect of IS on the proliferation of rat VSMCs by 4-[3-[4-Iodophenyl]-2-4(4-nitrophenyl)-2H-5-tetrazolio-1,3-benzene disulfonate] **proliferation assay.** Growth-arrested VSMCs were stimulated by IS and PDGF for 24 h. 4-[3-[4-Iodophenyl]-2-4(4-nitrophenyl)-2H-5-tetrazolio-1,3-benzene disulfonate] was added for the last 4 h. PDGF (10 ng/ml) was used as a positive control. Absorbance was measured by an enzyme-linked immunosorbent assay reader. Values are mean ± s.e.m. ($n = 8$). *$P < 0.05$ compared with the vehicle.

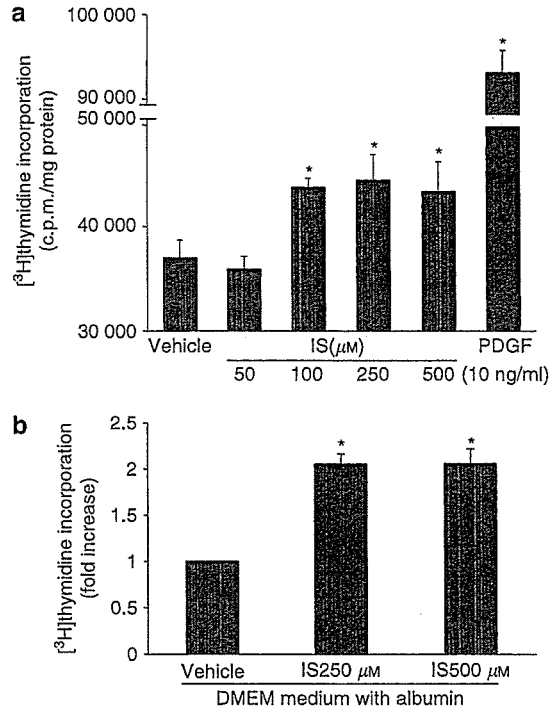

Figure 2 | Effect of IS on the proliferation of rat VSMCs assessed by DNA synthesis. (**a**) Growth-arrested VSMCs were stimulated by IS and PDGF for 24 h. [^{3}H]Thymidine was added for the last 6 h. PDGF (10 ng/ml) was used as a positive control. (**b**) Effect of IS on the proliferation of rat VSMCs in the presence of 4 g/dl albumin in the medium assessed by DNA synthesis. Values are mean ± s.e.m. ($n = 8$). *$P < 0.05$ compared with the vehicle.

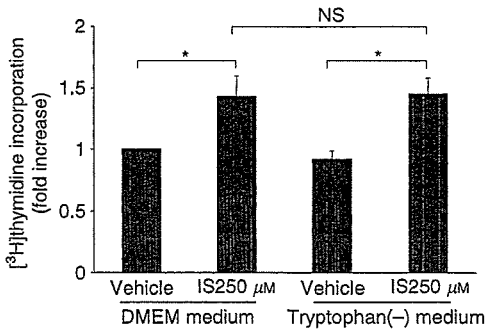

Figure 3 | Effect of the removal of tryptophan on IS-induced increase of DNA synthesis in rat VSMCs. Growth-arrested VSMCs were incubated for 24 h in DMEM or tryptophan (–) medium with or without IS (250 μM). [^{3}H]Thymidine was added for the last 6 h. Values are mean ± s.e.m. ($n = 8$). *$P < 0.05$ compared with vehicle.

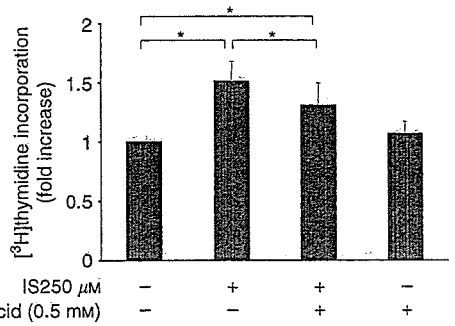

Figure 4 | Effect of probenecid on IS-induced increase of DNA synthesis in rat VSMC. Growth-arrested VSMCs were pretreated for 1 h with probenecid (0.5 mM) and then stimulated by IS (250 μM) for 24 h. Values are mean ± s.e.m. ($n = 8$). *$P < 0.05$.

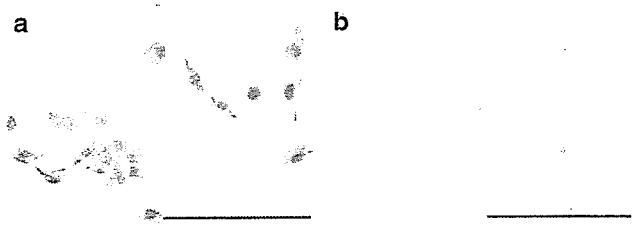

Figure 5 | Immunohistochemistry of rat OAT3 in rat VSMCs. (**a**) VSMCs were stained with polyclonal antibodies against rat OAT3 (**b**) There was no staining in the negative control with rabbit immunoglobulin fraction. Bar = 200 μm.

activation of p44/42 MAPK in VSMCs. As plasma concentration of IS in hemodialysis patients is reported to be about 250 μM,[5] we selected this dose for the following experiments. IS at 250 μM induced p44/42 MAPK phosphorylation in the cells, with a maximal intensity at 5 min (Figure 6). To confirm that the p44/42 MAPK pathway was actually involved in the IS-induced mitogenesis, we pretreated VSMCs with 10 μM PD98059, an MAPK/ERK kinase inhibitor,[14] to inhibit the pathway. The IS-induced phosphorylation was significantly inhibited by PD98059 (Figure 7). We further evaluated the effect of pretreatment with PD98059 at the same dose on the increase in IS-induced [3H]thymidine incorporation. PD98059 inhibited the increase in DNA synthesis by IS, whereas PD98059 alone had no effect on DNA synthesis (Figure 8).

IS increases mRNA expressions of PDGF-C chain and PDGF-β receptor

To discuss the mechanisms of IS-induced proliferation of VSMC, we evaluated the mRNA expressions of PDGF-A and -C chains, and PDGF-β receptor by real-time PCR. We found that mRNA expressions of PDGF-C chain and PDGF-β receptor were significantly increased by the addition of IS (Figure 9). Therefore, the increased expressions by IS are partly involved in the mechanism of IS-induced VSMC proliferation.

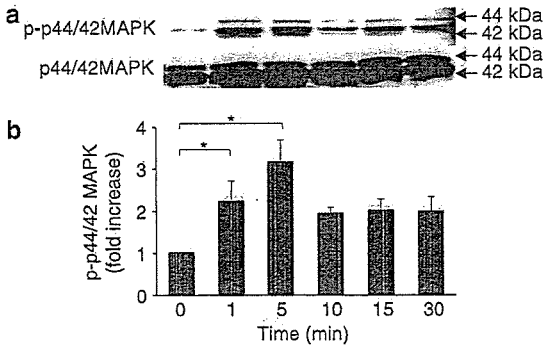

Figure 6 | Effect of IS on p44/42 MAPK phosphorylation. Growth-arrested VSMCs were stimulated by IS (250 μM) for the indicated times. (**a**) Representative immunoblots are shown with antibodies that recognize phosphorylated p44/42 MAPK and total p44/42 MAPK. (**b**) Densitometric analysis of phosphorylated p44/42 MAPK. Values are mean ± s.e.m. ($n = 5$). *$P < 0.05$.

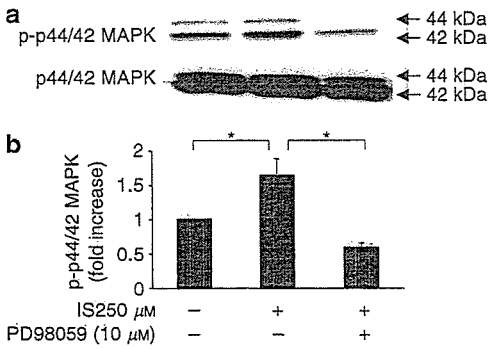

Figure 7 | Effect of PD98059 on IS-induced phosphorylation of p44/42 MAPK. Growth-arrested VSMCs were pretreated with PD98059 (10 μM) for 1 h and then stimulated by IS (250 μM) for 5 min. (**a**) Representative immunoblots are shown with antibodies that recognize phosphorylated p44/42 MAPK and total p44/42 MAPK. (**b**) Densitometric analysis of phosphorylated p44/42 MAPK. Values are mean ± s.e.m. ($n = 5$). *$P < 0.05$.

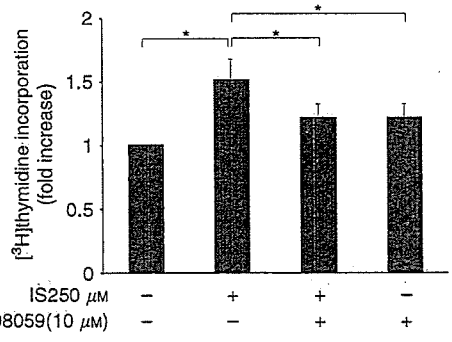

Figure 8 | Effect of PD98059 on IS-induced proliferation of rat VSMCs assessed by DNA synthesis. Growth-arrested VSMCs were pretreated for 1 h with PD98059 (10 μM) and then stimulated with IS (250 μM) for 24 h. Values are mean ± s.e.m. ($n = 8$). *$P < 0.05$.

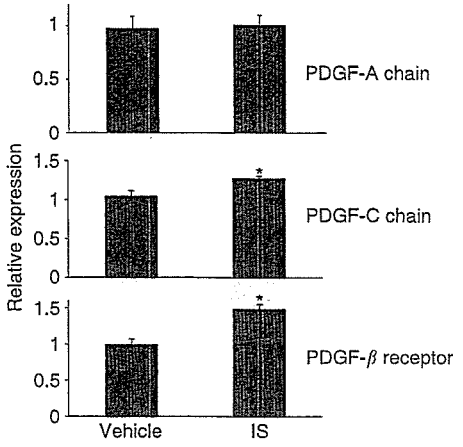

Figure 9 | Effect of IS on mRNA expressions of PDGF-A and -C chains and PDGF-β receptor. Growth-arrested VSMCs were stimulated with IS (250 μM) for 6 h and then total RNA was isolated. Real-time quantitative PCR was performed as described in Materials and Methods. Values are mean ± s.e.m. of two identical samples performed in at least triplicate ($n = 4$ in each). *$P < 0.05$ compared with the vehicle.

DISCUSSION

It is known that IS is a protein-bound uremic toxin that accelerates the progression of renal failure,[5] but data are limited about its actions on other organs. A recent *in vitro* study has shown that IS has a suppressive effect on the repair of damage in human umbilical vein endothelial cells, suggesting that the agent is involved in endothelium dysfunction in renal failure.[10] The present study shows for the first time that IS directly promotes VSMC proliferation. This is the most important finding in the present study. Serum concentration of IS in patients with end-stage renal failure is about 250 μM,[5] which is compatible with that needed to stimulate the proliferation of rat VSMCs in this study. As the enhanced proliferation of VSMCs in vascular walls is believed to promote hypertrophy of arteries, it is possible that VSMC proliferation induced by IS is one of the causes of cardiovascular complications that occur in dialysis patients with a high serum IS.

As IS is known to be transported by OATs on tubular cell membranes, the effect of probenecid, an inhibitor and substrate of OATs, on VSMC proliferation was investigated. In this experiment, we found that probenecid had an inhibitory effect on the proliferation of VSMCs. We also confirmed the presence of OAT3 in VSMCs by immunostaining. These findings suggest that IS is at least in part taken into VSMCs via OAT. Proliferation of VSMCs plays some role in the development of hypertension and arteriosclerosis,[19] and the p44/42 MAPK pathway is thought to be the intracellular signaling pathway involved in the proliferation of VSMCs.[13] When we evaluated the involvement of MAPK in the effect of IS on VSMCs, we found that pretreatment of VSMCs with PD98059, an inhibitor of MAPK, caused inhibition of VSMC proliferation. We also found that IS induced p44/42 MAPK phosphorylation, which was inhibited by PD98059. These findings indicate that the p44/42 MAPK pathway is involved in the induction of VSMC proliferation by IS.

In the present study, serum was not used in experiments examining the effects of IS stimulation, although no significant difference was found between the degrees of VSMC proliferation in serum with and without IS (data not shown). However, serum contains various growth factors, some of which might have a strong proliferative effect in addition to IS on VSMCs. Indeed, we found that the mRNA expressions of PDGF-C chain and PDGF-β receptor were increased by IS. Therefore, the increased expressions by IS are partly involved in the mechanism of IS-induced VSMC proliferation. The culture medium used in the present study contained tryptophan, a precursor of IS, but the possibility that the presence of tryptophan in the medium affected the results was ruled out by comparison of results of experiments using a medium containing tryptophan and a medium from which tryptophan had been removed.

The mechanisms by which IS induces proliferation of VSMC and activation of MAPK are not known. Uric acid has also been reported to be a uremic toxin that induces proliferation of VSMCs. Rao *et al.*[18] reported that uric acid induces proliferation of VSMCs by promoting the production of PDGF-A chain, and Johnson *et al.*[20,21] reported that uric acid is taken up by VSMCs via an OAT. As a potential mechanism for VSMC proliferation, uric acid, after being taken into VSMCs, activates MAPK and induces the production of cyclooxygenase-2 and the expression of PDGF-A chain, -C chain, and PDGF-α receptor mRNA.[20] We found that the induction of VSMC proliferation by IS was inhibited by probenecid and that MAPK was involved in the induction of VSMC proliferation by IS. Therefore, the mechanism of IS-induced VSMC proliferation might be similar to that of uric acid. To our knowledge, other protein-bound uremic toxins that have been shown to induce VSMC proliferation *in vitro* are homocysteine[22] and leptin.[23] Further study is needed to determine whether MAPK activation by IS is mediated by various growth factor receptors on the cell membrane surface or by an as yet unidentified receptor. To understand the pathophysiology of cardiovascular disease in end-stage renal disease patients, the effect of IS on other cell types of blood vessels and their crosstalk must be evaluated in the future.

In summary, the present *in vitro* study shows for the first time that IS directly induces cell proliferation of rat VSMC. Concentration of IS required to induce VSMC proliferation is similar to its blood concentration in patients on maintenance dialysis. Part of the action of IS on VSMC is mediated by OAT3, and the induction of VSMC proliferation by MAPK activation caused by IS. Increases of mRNA expressions of PDGF-C chain and PDGF-β receptor are also involved in the phenomenon. This might be one of the mechanisms underlying the progression of atherosclerotic lesions in end-stage renal disease patients.

MATERIALS AND METHODS

Materials

A p44/42 MAPK assay kit, including anti-p44/42 MAP kinase and anti-phospho-p44/42 MAP kinase (Thr202/Try204) antibodies, was purchased from Cell Signaling Technology (Beverly, MA, USA). A Cell Counting Kit was purchased from DOJINDO Laboratories (Kumamoto, Japan). [^{3}H]Thymidine was purchased from Perkin Elmer Life Science (Boston, MA, USA). Anti-rat OAT3 polyclonal antibody was purchased from TransGenic Inc. (Kumamoto, Japan). All other materials including IS were purchased from Sigma (St Louis, MO, USA). IS was dissolved with distilled water as vehicle in all experiments.

Cell culture

VSMCs were isolated from the aortas of male Sprague–Dawley rats (150–200 g) as previously described.[13] In brief, VSMCs were maintained in Dulbecco's modified Eagle's medium (DMEM) supplemented with 10% fetal bovine serum (FBS) (ICN Biomedicals, Osaka, Japan), 100 U/ml penicillin, and 100 mg/ml streptomycin (Life Technology Inc., Rockville, MD, USA) in a 5% CO_2 incubator at 37°C. VSMCs at 70–80% confluence were growth-arrested by incubation in DMEM with 0.5% FBS for 48 h. The cells were used between passages 3 and 8. VSMCs were identified by their typical hill and valley morphology and by indirect immunofluorescent staining for α-smooth muscle actin (R&D Systems Inc., Minneapolis, MN, USA). We measured endotoxin concentration in the medium by limulus amebocyte lysate method (Wako Pure Chemical Industries, Osaka, Japan) and found that it was under the detection limit, which strongly indicated the absence of lipopolysaccharide in the medium.

Cell proliferation assay

VSMC proliferation was assessed using the Cell Counting Kit.[24] The cells were seeded at a density of 5×10^3 cells/well on 96-well culture plates in DMEM with 10% FBS for 72 h. After serum starvation for 48 h in DMEM with 0.5% FBS, the cells were stimulated by IS or PDGF as a positive control for 24 h. For the final 4 h of incubation, 4-[3-[4-Iodophenyl]-2-4(4-nitrophenyl)-2H-5-tetrazolio-1,3-benzene disulfonate] was added to each well and the absorbance was measured at 450 nm with a reference wavelength of 650 nm using a microplate spectrophotometer system (SOFTmax PRO, Molecular Devices Corporation, Sunnyvale, CA, USA). The difference of absorbance between 450 and 650 nm was regarded as the cell proliferation.

[^{3}H]Thymidine incorporation

The cells were seeded on 24-well culture plates, allowed to grow to 70–80% confluence, and then growth-arrested by incubation in DMEM with 0.5% FBS for 48 h. The cells were incubated for 24 h, and [^{3}H]thymidine (1 μCi/ml; specific activity, 79 Ci/mmol) was added to for the last 6 h of the incubation period. The cells were then washed three times with phosphate-buffered saline, treated with ice-cold 10% trichloroacetic acid at 4°C for 15 min, and washed with phosphate-buffered saline. The acid-insoluble material was dissolved in 0.5 ml of 0.3 N NaOH. The protein content was measured by a DC Protein Assay (Bio-Rad, Hercules, CA, USA), and radioactivity was determined by using a liquid scintillation counter (Aloka, Japan).

Western blot analysis

Growth-arrested cells cultured in 100-mm dishes were stimulated by 250 μM IS for the indicated times. For the inhibitor studies, cells were pretreated for 1 h with PD98059 (10 μM), an MAPK/ERK kinase inhibitor.[14] The cells were washed with ice-cold phosphate-buffered saline and lysed in 400 μl of lysis buffer (1% Triton, 20 mM Tris-HCl (pH 7.5), 150 mM NaCl, 1 mM Na_2EDTA, 1 mM ethyleneglycol tetraacetate, 2.5 mM sodium pyrophosphate, 1 mM β-glycerophosphate, 1 mM Na_3VO_4, 1 μg/ml L-leupeptin, 1 mM phenylmethylsulfonyl fluoride) for 30 min at 4°C. The cell lysates were centrifuged for 15 min at 15 000 *g* and the supernatants were collected. Equal amounts of protein (20 μg) were separated by 10% sodium dodecyl sulfate-polyacrylamide gel electrophoresis, and electrophoretically transferred to polyvinylidine difluoride membranes (Invitrogen Corp., Carlsbad, CA, USA). The membranes were blocked for 1 h at room temperature with Tris-buffered saline containing 0.05% Tween 20 (TBS-T) and 5% bovine serum albumin. After washing with TBS-T, the membranes were incubated overnight with phospho-p44/42 MAPK (Thr202/Tyr204) antibody (1:1000) or p44/42 MAPK antibody (1:1000) (Cell Signaling Technology, Beverly, MA, USA) at 4°C with gentle shaking. The primary antibodies were detected using horseradish peroxidase-conjugated goat antirabbit IgG and visualized by enhanced chemiluminescence Western blotting reagents (Amersham Biosciences, Buckinghamshire, UK). Band intensity was analyzed using KODAK 1D Image Analysis Software (KODAK, Rochester, NY, USA).

Immunohistochemical staining

Immunostaining of OAT3 in rat VSMCs was performed by the labeled streptavidin biotin (LSAB) method using a DAKO LSAB Kit (Dako, Carpinteria, CA, USA). Briefly, VSMCs were cultured on eight-well Lab-Tek chamber slides (Nalge Nunc International) and fixed with paraformaldehyde lysine periodate solution (containing 0.01 M $NaIO_4$, 0.075 M lysine, 0.0375 M phosphate buffer with 2% paraformaldehyde; pH 6.2) for 1 h at 4°C. After fixation, the cells were permeabilized in 0.1% Triton X-100 in phosphate-buffered saline for 5 min and incubated with 3% hydrogen peroxide for 30 min to suppress endogenous peroxidase activity and then with blocking solution for 10 min. The cells were incubated with a polyclonal antibody against rat OAT3[8] (1:20) at 4°C overnight. The negative controls were treated with the rabbit immunoglobulin fraction (Dako, Carpinteria, CA, USA). After rinsing with TBS-T, the cells were incubated with a biotinylated link antibody against rabbit immunoglobulin for 30 min. The cells were washed with TBS-T and incubated with horseradish peroxidase-conjugated streptavidine solution for 30 min. Horseradish peroxidase labeling was detected using a peroxidase substrate diaminobenzidine, and then counterstaining was performed with hematoxylin.

RNA extraction and real-time quantitative PCR

The isolation of total RNA was achieved using the RNeasy Mini Kit (Quiagen, Valencia, CA, USA). Reverse transcription was performed with 1.2 μg of total RNA, random hexamer primers, and RevertAid M-MuLV reverse transcriptase (Fermentas, Hanover, MD, USA). The resulting cDNA equivalent to 60 ng of RNA was used for real-time quantitative PCR in the ABI Prism 7700 sequence detection system (Applied Biosystems, Foster City, CA, USA) as previously described.[25] All of the specific sets of primers and TaqMan probes in the present study were obtained from Applied Biosystems (Assays-on-Demand Gene Expression Products and TaqMan Rodent GAPDH Control Reagants). All primer sets but that of TaqMan Rodent GAPDH Control Reagents were designed to be located in two exons to avoid amplification of potentially contaminating

genomic DNA. To control the variation in the amount of DNA available for PCR in the different samples, gene expressions of the target sequence were normalized in relation to the expression of an endogenous control, glyceraldehyde-3-phosphate dehydrogenase. As the efficiency of the target amplification was approximately equal to that of the glyceraldehyde-3-phosphate dehydrogenase amplification, data were analyzed using the comparative threshold cycle method.[26] Because the intra- and interassay coefficients of variation of the relative expression values were $<20\%$, we considered the mean relative values of less than 0.8 or more than 1.2 to be significant in this study.

Statistics

The results are expressed as the mean $\pm$ s.e.m. Data were analyzed by the unpaired Student's *t*-test or by one-way analysis of variance combined with Fisher's protected least significant difference using personal computer with StatView version 5.0 (SAS Institute, Cary, NC, USA). Differences with $P<0.05$ were considered to be significant.

ACKNOWLEDGMENTS

We thank Mrs Yuko Watanabe for technical assistance. This study was supported in part by grants from Research on Advanced Medical Technology, Health and Labor Sciences, and Grant program for Promoting Advancement of Academic Research at Private Universities, Ministry of Education, Culture, Science and Technology of Japan.

REFERENCES

1. Foley RN, Parfrey PS, Sarnak MJ. Clinical epidemiology of cardiovascular disease in chronic renal disease. *Am J Kidney Dis* 1998; **32**: S112–S119.
2. Anavekar NS, Pfeffer MA. Cardiovascular risk in chronic kidney disease. *Kidney Int Suppl* 2004; **66**(Suppl 92): S11–S15.
3. Lesaffer G, De Smet R, Lameire N *et al.* Intradialytic removal of protein-bound uraemic toxins: role of solute characteristics and of dialyser membrane. *Nephrol Dial Transplant* 2000; **15**: 50–57.
4. Vanholder R, Glorieux G, De Smet R *et al.* New insights in uremic toxins. *Kidney Int Suppl* 2003; **63**(Suppl 84): S6–S10.
5. Niwa T, Ise M. Indoxyl sulfate, a circulating uremic toxin, stimulates the progression of glomerular sclerosis. *J Lab Clin Med* 1994; **124**: 96–104.
6. Niwa T, Takeda N, Tatematsu A *et al.* Accumulation of indoxyl sulfate, an inhibitor of drug-binding, in uremic serum as demonstrated by internal-surface reversed-phase liquid chromatography. *Clin Chem* 1988; **34**: 2264–2267.
7. Niwa T. Renal cell metabolism. In: Massry SG, Glassock RJ (eds). *Textbook of Nephrology*, 4th edn, Williams and Wilkins: Philadelphia, 2001, pp 1269–1272.
8. Enomoto A, Takeda M, Tojo A *et al.* Role of organic anion transporters in the tubular transport of indoxyl sulfate and the induction of its nephrotoxicity. *J Am Soc Nephrol* 2002; **13**: 1711–1720.
9. Miyazaki T, Ise M, Hirata M *et al.* Indoxyl sulfate stimulates renal synthesis of transforming growth factor-beta 1 and progression of renal failure. *Kidney Int Suppl* 1997; **63**: S211–S214.
10. Dou L, Bertrand E, Cerini C *et al.* The uremic solutes p-cresol and indoxyl sulfate inhibit endothelial proliferation and wound repair. *Kidney Int* 2004; **65**: 442–451.
11. Blenis J. Signal transduction via the MAP kinases: proceed at your own RSK. *Proc Natl Acad Sci USA* 1993; **90**: 5889–5892.
12. Ito C, Yamamoto H, Furukawa Y *et al.* Role of cyclins in cAMP inhibition of glomerular mesangial cell proliferation. *Clin Sci (London)* 2004; **107**: 81–87.
13. Akimoto T, Kusano E, Ito C *et al.* Involvement of erythropoietin-induced cytosolic free calcium mobilization in activation of mitogen-activated protein kinase and DNA synthesis in vascular smooth muscle cells. *J Hypertens* 2001; **19**: 193–202.
14. Graf K, Xi XP, Yang D *et al.* Mitogen-activated protein kinase activation is involved in platelet-derived growth factor-directed migration by vascular smooth muscle cells. *Hypertension* 1997; **29**: 334–339.
15. Bokemeyer D, Schmitz U, Kramer HJ. Angiotensin II-induced growth of vascular smooth muscle cells requires an Src-dependent activation of the epidermal growth factor receptor. *Kidney Int* 2000; **58**: 549–558.
16. Ito C, Kusano E, Furukawa Y *et al.* Modulation of the erythropoietin-induced proliferative pathway by cAMP in vascular smooth muscle cells. *Am J Physiol Cell Physiol* 2002; **283**: C1715–C1721.
17. Brown JC, Rosenquist TH, Monaghan DT. ERK2 activation by homocysteine in vascular smooth muscle cells. *Biochem Biophys Res Commun* 1998; **251**: 669–676.
18. Rao GN, Corson MA, Berk BC. Uric acid stimulates vascular smooth muscle cell proliferation by increasing platelet-derived growth factor A-chain expression. *J Biol Chem* 1991; **266**: 8604–8608.
19. Gibbons GH, Dzau VJ. Molecular therapies for vascular diseases. *Science* 1996; **272**: 689–693.
20. Johnson RJ, Kang DH, Feig D *et al.* Is there a pathogenetic role for uric acid in hypertension and cardiovascular and renal disease? *Hypertension* 2003; **41**: 1183–1190.
21. Han L, Kanellis J, Li P *et al.* The evidence for a functional organic anion transporter in vascular smooth muscle cells. *J Am Soc Nephrol* 2002; **13**: 329A.
22. Tsai JC, Perrella MA, Yoshizumi M *et al.* Promotion of vascular smooth muscle cell growth by homocysteine: a link to atherosclerosis. *Proc Natl Acad Sci USA* 1994; **91**: 6369–6373.
23. Oda A, Taniguchi T, Yokoyama M. Leptin stimulates rat aortic smooth muscle cell proliferation and migration. *Kobe J Med Sci* 2001; **47**: 141–150.
24. Motojima M, Hosokawa A, Yamato H *et al.* Uraemic toxins induce proximal tubular injury via organic anion transporter 1-mediated uptake. *Br J Pharmacol* 2002; **135**: 555–563.
25. Ando H, Tsuruoka S, Yamamoto H *et al.* Effects of pravastatin on the expression of ATP-binding cassette transporter A1. *J Pharmacol Exp Ther* 2004; **21**: 21.
26. Su YR, Linton MF, Fazio S. Rapid quantification of murine ABC mRNAs by real time reverse transcriptase-polymerase chain reaction. *J Lipid Res* 2002; **43**: 2180–2187.

Eur J Clin Pharmacol
DOI 10.1007/s00228-006-0142-y

PHARMACOEPIDEMIOLOGY AND PRESCRIPTION

Shuichi Tsuruoka · Atsuhiro Kawaguchi · Kazuhiro Harada · Akio Fujimura

Favorable effect on postgraduate clinical practice of a drug-interaction exercise for undergraduate students

Received: 9 February 2006 / Accepted: 6 April 2006

Abstract *Aim:* Undergraduate students in Jichi Medical School participated in a laboratory exercise investigating the furosemide–probenecid interaction at the end of their clinical pharmacology (CP) course. The aim of this study was to determine whether they learned to recognize drug interactions better than students who did not take such a course. *Methods:* We conducted a postal survey of physicians who had graduated from Jichi Medical School or from other medical schools without a CP course including the exercise. Questions were asked concerning: (1) the recognition of furosemide–probenecid and nine other drug interactions, and (2) the need to anticipate drug interactions and their adverse effects before writing prescriptions. *Results:* The degree of the recognition of all drug interactions, and the percentage of physicians who responded that knowledge of drug interactions and adverse effects were essential before writing prescriptions, were significantly greater in physicians who had taken an undergraduate CP course than in those who had not. *Conclusions:* CP courses with specific laboratory exercises on drug interactions lead future physicians to recognize drug interactions and their adverse effects.

Keywords Drug-interaction exercise · Postgraduate clinical practice · Undergraduate course

Introduction

During the last decade, dramatic changes in medical education have occurred worldwide because of dissatisfaction with the way in which doctors were being trained. A traditional passive approach has been replaced by a more active approach. Educational reform has also taken place in the fields of basic and clinical pharmacology [1–7].

The clinical pharmacology (CP) course in the Jichi Medical School is a compulsory course and consists of 16 lectures concerning the core knowledge of CP, such as clinical pharmacokinetics, adverse drug reactions, and drug interactions. At the end of the course, undergraduate students participate in a laboratory exercise investigating the furosemide–probenecid interaction, as described previously [8]. In brief, students are randomly assigned to one of three groups in a double-blind fashion: (1) placebo plus 20 mg of furosemide; (2) 250 mg of probenecid plus 20 mg of furosemide; and (3) 1,000 mg of probenecid plus 20 mg of furosemide. They take probenecid or its placebo 1 h before furosemide. Urine volume and urinary sodium excretion are measured for 3 h after they take furosemide.

We analyzed data obtained for 5 years (1995–1999) and found that the furosemide–probenecid interaction exercise was easy to perform, reproducible, and safe [8]. In addition, more than 80% of the students considered the exercise to be useful. Based on these observations, we hypothesized that the CP course with the furosemide–probenecid laboratory exercise would motivate students to recognize drug interactions and their adverse effects. To evaluate this hypothesis, we conducted a postal survey of physicians who had graduated from Jichi Medical School or other medical schools without a CP course.

Methods

Physicians who had been in clinical practice for 3–7 years participated in this study. A questionnaire was sent by mail to 527 graduates of Jichi Medical School whose mailing addresses were available on file. Each was asked to provide copies of the questionnaire to colleagues who had graduated from other medical schools and worked at the same hospital. Their colleagues were asked whether they took a CP course during their undergraduate education.

As shown in Table 1, questions were asked concerning the recognition of the furosemide–probenecid interaction

S. Tsuruoka (✉) · A. Kawaguchi · K. Harada · A. Fujimura
Department of Clinical Pharmacology, Jichi Medical School,
3311 Yakushiji, Shimotsuke,
Tochigi, 329-0498, Japan
e-mail: tsuru@jichi.ac.jp
Tel.: +81-285-587387
Fax: +81-285-447562

t1.1 **Table 1** List of questions

t1.2 No.	Drug interaction	Recognition
t1.3 1	Digoxin–verapamil	A B C
t1.4 2	Tetracycline–aluminum	A B C
t1.5 3	Warfarin–aspirin	A B C
t1.6 4	Cisapride–clarithromycin	A B C
t1.7 5	Nifedipine–rifampicin	A B C
t1.8 6	Aspirin–sodium bicarbonate	A B C
t1.9 7	Furosemide–probenecid	A B C
t1.10 8	Ciclosporine–grapefruit juice	A B C
t1.11 9	Quinolones–NSAIDs	A B C
t1.12 10	HMG CoA reductase inhibitors–clofibrates	A B C

I. Do you recognize the following drug interactions?
A: yes, and understand its mechanism; B: yes, but do not understand its mechanism; C: no
II. Is the knowledge of drug interactions and adverse effects essential for prescribing drugs?
1. Drug interactions: yes no
2. Drug-related adverse effects: yes no

and nine clinically important drug interactions documented in National drug formulary by the Ministry of Health, Labour and Welfare, Japan [9]. The possible answers were: (A) knew it and understood its mechanism; (B) knew it but did not understand its mechanism; or (C) did not know it. Respondents were also asked whether understanding drug interactions and their adverse effects was essential for prescribing drugs.

Because physicians who had graduated from Jichi Medical School participated in the furosemide–probenecid laboratory exercise, these respondents were divided into three groups: (I) knew the furosemide–probenecid interaction and understood its mechanism; (II) knew the drug interaction but did not understand its mechanism; (III) did not know the drug interaction. Respondents who had graduated from other medical schools and did not participate in CP courses or laboratory exercises during their undergraduate education belonged to group IV.

Data were analyzed by chi-square or Kruskal-Wallis tests as appropriate. The level of significance was set at $P<0.05$.

Results

Of the 527 survey recipients, 357 (68%) responded (group I=139, group II=118, group III=100). In addition, 126 physicians who graduated from other medical schools responded; because 23 of them took a CP course with laboratory exercises (other than drug-interaction exercises) during their undergraduate education, they were not included (group IV=103). Thirty-five (34%) doctors in group IV recognized the furosemide–probenecid interaction. The various medical specialties of respondents are shown in Table 2; specialty did not differ significantly between the groups who took a CP course (I + II + III) and the group that did not (IV; $P>0.05$) or among groups I, II, and III ($P>0.40$).

There was a significant difference between groups I, II, and III and group IV with regard to recognition of all drug interactions (Fig. 1). Among groups I, II, and III, significant differences were also observed in the degree of the recognition of eight drug interactions (except quinolones–NSAIDs). In these eight drug interactions, the degree of recognition was greater in group I than in groups II and III. Physicians in group II recognized more drug interactions than did those in group III, except for the tetracycline–aluminium interaction.

The percentages of physicians who responded that understanding drug interactions and their adverse effects was essential for prescribing drugs were significantly greater in the group with the CP course (I + II + III) than in the group without (IV; Table 3).

t2.1 **Table 2** Medical specialty in each group

	Number (and %) in each group			
t2.2 Specialty	I	II	III	IV
t2.3 Medicine	81 (58%)	65 (55%)	50 (50%)	43 (42%)
t2.4 Surgery	24 (17%)	14 (12%)	20 (20%)	18 (18%)
t2.5 Pediatrics	10 (7%)	7 (6%)	4 (4%)	3 (3%)
t2.6 Gynecology	4 (3%)	7 (6%)	4 (4%)	6 (6%)
t2.7 Other	20 (15%)	25 (21%)	22 (22%)	32 (31%)
t2.8 No answer	0 (0%)	0 (0%)	0 (0%)	1 (0%)
t2.9 Total (male/female)	139 (112/27)	118 (95/23)	100 (79/21)	103 (85/18)
t2.10 Age (mean±SE)	30.2±2.2	29.8±2.5	30.9±2.0	31.0±2.2

(I) Doctors who knew the furosemideprobenecid interaction, understood its mechanism and participated in CP courses or laboratory exercise in Jichi Medical School; (II) octors who knew the drug interaction but did not understand its mechanism and participated in CP courses or laboratory exercise in Jichi Medical School; (III) doctors who did not know the drug interaction and participated in CP courses or laboratory exercise in Jichi Medical School; (IV) doctors who graduated from other medical schools and did not participate in CP courses or laboratory exercises during their undergraduate education

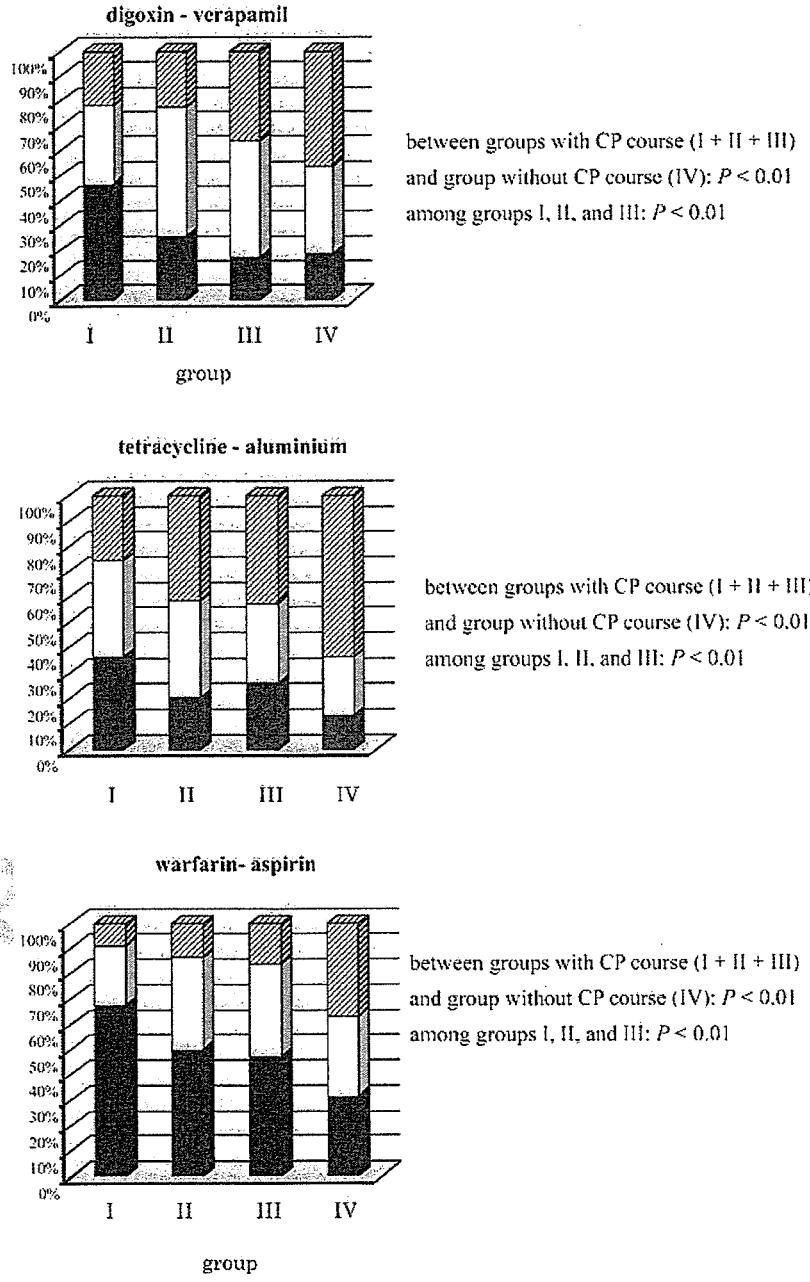

Fig. 1 Recognition of clinically important drug interactions that were documented by the Ministry of Health, Labour and Welfare, Japan. Sample sizes of groups I, II, III, and IV were 139, 118, 100, and 103, respectively. (I) Doctors who knew the furosemide–probenecid interaction, understood its mechanism and participated in CP courses or laboratory exercise in Jichi Medical School; (II) doctors who knew the drug interaction but did not understand its mechanism and participated in CP courses or laboratory exercise in Jichi Medical School; (III) doctors who did not know the drug interaction and participated in CP courses or laboratory exercise in Jichi Medical School; (IV) doctors who graduated from other medical schools and did not participate in CP courses or laboratory exercises during their undergraduate education

a: knew it and understood its mechanism

b: knew it but did not understand its mechanism

c: did not know it

Discussion

At the beginning of the 1990s, it was recognized that the inhibition of terfenadine metabolism by erythromycin and ketoconazole led to serious adverse effects [8], thus highlighting the importance of physicians recognizing drug interactions. Subsequently, the U.S. Food and Drug Administration has published guidelines for studies of in vitro and in vivo drug interactions [10, 11]. To avoid serious drug-related adverse effects in patients, it is important to improve the system of transmitting information about drug interactions to physicians [12]. It is also necessary that undergraduate students acquire the knowledge and understanding of drug interactions during CP courses. However, for medical students to develop an attitude that will lead them to assess and estimate potential drug interactions before prescribing drugs, we think it is important that the students themselves experience a drug interaction.

The drug interaction between furosemide and probenecid is well known. Both furosemide and probenecid are secreted in urine by the renal organic anion transport system [13, 14]. Therefore, when these agents are coadministered, probenecid reduces the renal secretion of furosemide and subsequent diuretic effects. For more than 15 years at Jichi Medical School, we have performed a laboratory exercise of the furosemide–probenecid interaction at the end of the CP course for undergraduate students.

Fig. 1 (continued)

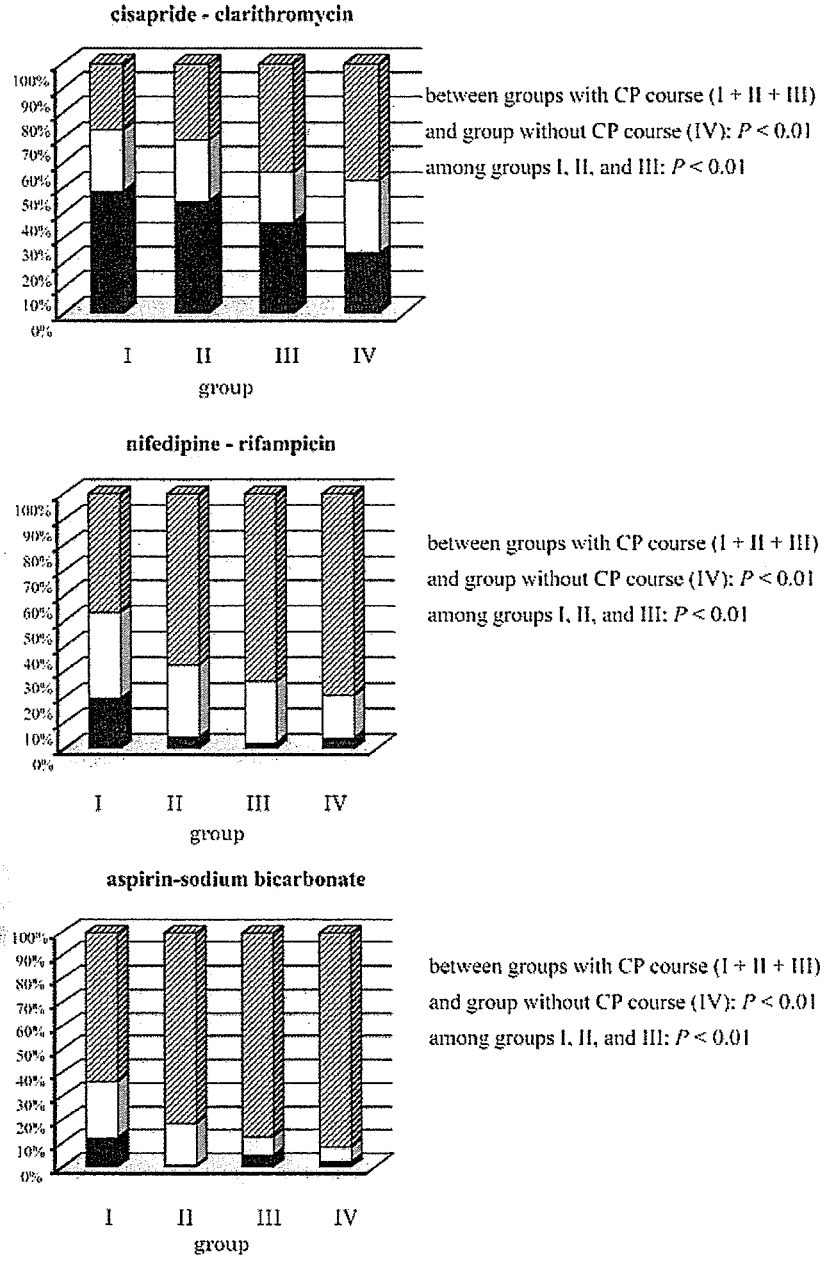

Recently, we analyzed data obtained from 1995 to 1999 and found that the exercise was easy to perform, reproducible, and safe [8].

In this study, we surveyed physicians who had been prescribing drugs for 3–7 years, and we evaluated the effect of the CP course including the furosemide–probenecid exercise on their recognition of clinically important drug interactions. The percentage of physicians who responded that knowledge of drug interactions was essential for prescribing drugs and the degree of recognition of ten drug interactions was significantly greater in the group which had taken an undergraduate CP course than in those who had not. In addition, the percentage of doctors who thought that the knowledge of drug-related adverse effects was essential before writing a prescription was also significantly greater in the group which had taken the CP course. Based on these results, we think that a CP course including the furosemide–probenecid laboratory exercise provides a good opportunity for active learning of drug interactions and adverse reactions in patients.

In general, among physicians who had taken the CP course, the degree of the recognition of drug interactions was group I (knew the furosemide–probenecid interaction and understood its mechanism) > group II (knew the drug interaction but did not understand its mechanism) > group III (did not know the drug interaction). These findings suggest that both the recognition of potential drug interactions as well as an understanding of the underlying

Fig. 1 (continued)

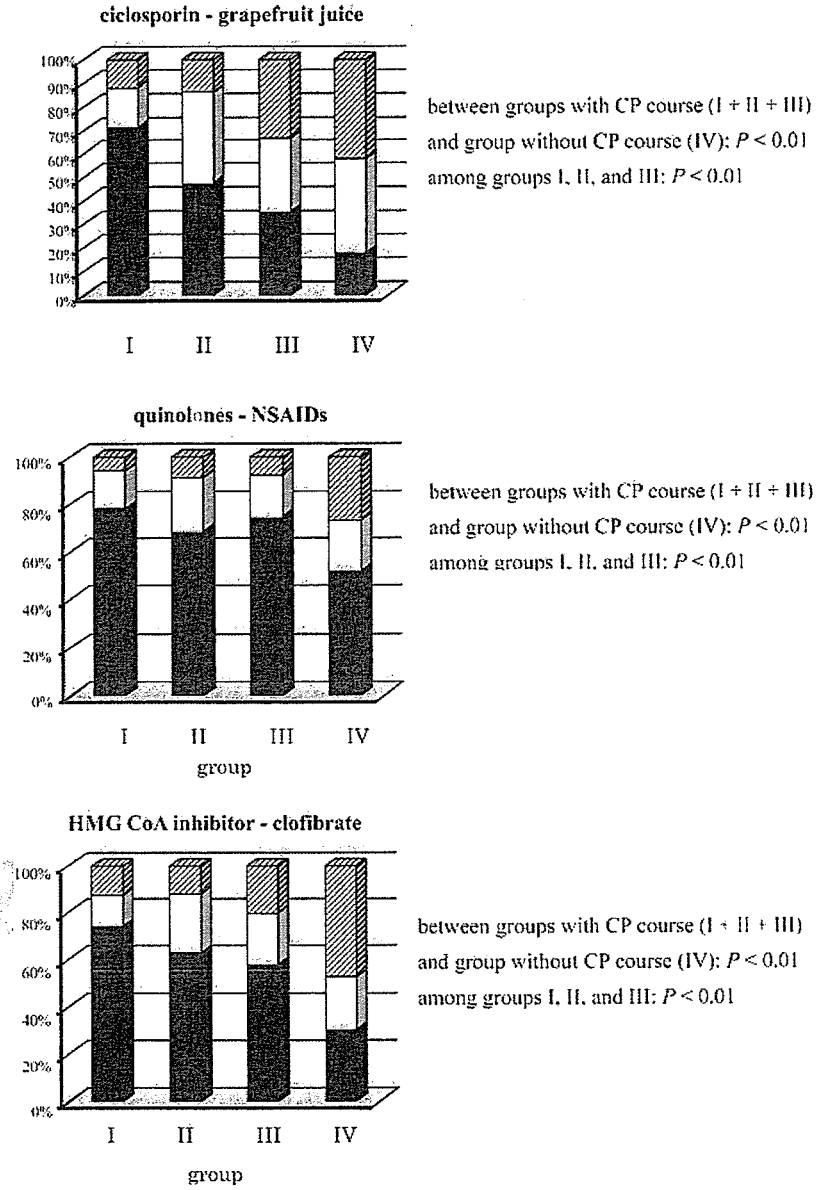

mechanisms are needed to prevent serious adverse effects in future clinical practice.

Because this study is based on a questionnaire survey, it is difficult to estimate the honesty of the responses, which is a limitation of the study. However, because we can assume that the incidence of dishonesty was evenly distributed in all groups, the results still indicated the effectiveness of the laboratory exercise in the undergraduate CP course. Another possible interpretation of the present results could be that the graduates of Jichi Medical School had greater knowledge about drug interaction whether they had done the laboratory exercise or not. However, we think that such a possibility is small because the degree of recognition in group I is greater than group II

Table 3 Percentage of physicians who responded that knowledge of drug interactions and adverse effects were essential for prescribing drugs

Knowledge	Group		
	With CP course (I + II + III) (*n*=357)	Without CP course (IV) (*n*=103)	*P*-value
Drug interactions	65%	45%	<0.01
Adverse effects	50%	39%	<0.05

and III (all were graduates from Jichi Medical School) as discussed in the previous paragraph.

In summary, this study showed that physicians who took a CP course including a drug-interaction laboratory exercise during their undergraduate education were more likely to recognize clinically important drug interactions. Through the personal experience of a drug interaction, undergraduate medical students will be more motivated to recognize drug interactions once in clinical practice.

References

1. Stichtenoth DO, Frolich JC (2004) Pregraduate teaching clinical pharmacology in Germany. Eur J Clin Pharmacol 60:225–229
2. Orme M, Frolich J, Vrhovac B (2002) Towards a core curriculum in clinical pharmacology for undergraduate medical students in Europe. Eur J Clin Pharmacol 58:635–640
3. Vlahovic Palcevski V, Vitezic D, Zupan G, Simonic A (1998) Education in clinical pharmacology at the Rijeka School of Medicine, Croatia. Eur J Clin Pharmacol 54:685–689
4. Eroglu L, Uresin Y (2003) A model of pharmacology education: the experience of Istanbul medical faculty. J Clin Pharmacol 43:237–242
5. Smith CM (1997) Using student feedback on examination questions to promote fairness, item validity, and learning. J Clin Pharmacol 37:379–387
6. Michel MC, Bischoff A, Jakobs KH (2002) Comparison of problem-and lecture-based pharmacology teaching. Trends Pharmacol Sci 23:168–170
7. Whiting B, Holford NH, Begg EJ (2002) Clinical pharmacology: principles and practice of drug therapy in medical education. Br J Clin Pharmacol 54:1–2
8. Kawaguchi A, Sugimoto K, Ohmori M, Tsuruoka S, Harada K, Kitoh Y et al (2001) Furosemide-probenecid interaction as a laboratory exercise for undergraduate education in clinical pharmacology. Clin Pharmacol Ther 69:232–237
9. Quinn D, Day R (1997) Clinically important drug interactions. In: Speight T, Holford N (eds) Avery's drug treatment, 4th edn. Adis International, Auckland, pp 301–338
10. Guidance for Industry: drug metabolism/drug interactions in the drug development process. Studies in vitro. http://www.fda.gov/cder/guidance/clin3.pdf
11. Guidance for Industry: in vivo drug metabolism/drug interaction studies. Study design, data analysis, and recommendations for dosing and labeling. http://www.fda.gov/cder/guidance/2635fnl.pdf
12. Harada K, Fujimura A (2000) The need for improving information systems on drug interactions in Japan. Arch Intern Med 160:2063–2064
13. Honari J, Blair AD, Cutler RE (1977) Effects of probenecid on furosemide kinetics and natriuresis in man. Clin Pharmacol Ther 22:395–401
14. Pichette V, du Souich P (1996) Role of the kidneys in the metabolism of furosemide: its inhibition by probenecid. J Am Soc Nephrol 7:345–349

Am J Physiol Renal Physiol 291: F866–F873, 2006.
First published May 16, 2006; doi:10.1152/ajprenal.00027.2006.

Endothelin and nitric oxide mediate adaptation of the cortical collecting duct to metabolic acidosis

Shuichi Tsuruoka,[1] Seiji Watanabe,[2] Jeffrey M. Purkerson,[2] Akio Fujimura,[1] and George J. Schwartz[2]
[1]*Department of Pharmacology, Jichi Medical School, Tochigi, Japan; and* [2]*Department of Pediatrics, University of Rochester School of Medicine, Rochester, New York*

Submitted 25 January 2006; accepted in final form 10 May 2006

Tsuruoka, Shuichi, Seiji Watanabe, Jeffrey M. Purkerson, Akio Fujimura, and George J. Schwartz. Endothelin and nitric oxide mediate adaptation of the cortical collecting duct to metabolic acidosis. *Am J Physiol Renal Physiol* 291: F866–F873, 2006. First published May 16, 2006; doi:10.1152/ajprenal.00027.2006.—Endothelin (ET) and nitric oxide (NO) modulate ion transport in the kidney. In this study, we defined the function of ET receptor subtypes and the NO guanylate cyclase signaling pathway in mediating the adaptation of the rabbit cortical collecting duct (CCD) to metabolic acidosis. CCDs were perfused in vitro and incubated for 3 h at pH 6.8, and bicarbonate transport or cell pH was measured before and after acid incubation. Luminal chloride was reversibly removed to isolate H^+ and HCO_3^- secretory fluxes and to raise the pH of β-intercalated cells. Acid incubation caused reversal of polarity of net HCO_3^- transport from secretion to absorption, comprised of a 40% increase in H^+ secretion and a 75% decrease in HCO_3^- secretion. The ET_B receptor antagonist BQ-788, as well as the NO synthase inhibitor, N^G-nitro-L-arginine methyl ester (L-NAME), attenuated the adaptive decrease in HCO_3^- secretion by 40%, but only BQ-788 inhibited the adaptive increase in H^+ secretion. There was no effect of inactive D-NAME or the ET_A receptor antagonist BQ-123. Both BQ-788 and L-NAME inhibited the acid-induced inactivation (endocytosis) of the apical Cl^-/HCO_3^- exchanger. The guanylate cyclase inhibitor LY-83583 and cGMP-dependent protein kinase inhibitor KT-5823 affected HCO_3^- transport similarly to L-NAME. These data indicate that signaling via the ET_B receptor regulates the adaptation of the CCD to metabolic acidosis and that the NO guanylate cyclase component of ET_B receptor signaling mediates downregulation of Cl^-/HCO_3^- exchange and HCO_3^- secretion.

tubule microperfusion; endothelin receptor antagonist; nitric oxide synthase inhibitor; cyclic GMP; cyclic GMP-dependent protein kinase

ENDOTHELINS (ET) were first described as vasoactive peptides that regulate regional vascular tone by signaling cells in the cardiovascular system via members of the G protein-coupled receptor family (15a, 45). Since the early 1990s, it has become apparent that ET also regulates sodium-water balance and pH homeostasis in the kidney by directly signaling renal epithelial cells. ET promotes water diuresis by acting to inhibit the hydroosmotic action of vasopressin (22). Several studies implicate ET in the regulation of acid-base homeostasis in the proximal tubule (41) as well as the distal nephron (42, 43). ET modulates NHE3 activity in the proximal tubule and thereby regulation of proton secretion by this segment (13). In the distal nephron, ET-1 is abundantly expressed by collecting ducts (12), as are ET_B receptors (29). ET stimulates distal tubular acidification in the rat (42, 43), and the expression of ET in the kidney is stimulated by metabolic acidosis (44). Mice having a genetically disrupted ET_B receptor experience a more severe acidosis than normal mice in response to acid loading (13). However, a detailed assessment of the regulation of proton vs. bicarbonate transport in the cortical collecting duct (CCD) is lacking.

In many cases, the effects of ET on ion transport processes in nephron segments are mediated by the generation of nitric oxide (NO) resulting from activation of a NO synthase (NOS) (9, 10, 17). In vivo studies suggest that NO induces a natriuresis and diuresis, which is mediated by activation of guanylate cyclase. In the proximal tubule, Wang et al. (41) reported that tubules from neuronal NOS knockout mice exhibited lower fluid and HCO_3^- absorption rates compared with tubules from wild-type mice. Thus NO produced by neuronal NOS in the proximal tubule is likely to stimulate fluid and HCO_3^- absorption. In the CCD NO inhibits Na^+ absorption and vasopressin-stimulated osmotic water permeability (5, 17). The effect of NO on osmotic water permeability is blocked by guanylate cyclase and cGMP-dependent protein kinase (PKG) inhibitors, indicating that the effect of NO is mediated by activation of soluble guanylate cyclase and subsequent activation of PKG by cGMP (6, 17). This cascade results in inhibition of vasopressin-stimulated osmotic water permeability (6, 17).

In the thick ascending limb, endogenous NO inhibits chloride transport (20), and a comparable inhibition is observed using exogenous ET-1 (19). The ET effect is blocked by inhibiting NOS with N^G-nitro-L-arginine methyl ester (L-NAME) (19), suggesting that the effects of ET-1 are mediated by NOS in the thick ascending limb of Henle's loop (9).

NO also regulates pH homeostasis in the distal nephron. In freshly isolated CCDs, NO donors decrease bafilomycin-sensitive H^+-ATPase activity (31). Such inhibition is likely mediated by cGMP because cGMP analogs also inhibit H^+-ATPase activity (31). However, this finding would lead to an expectation of decreased H^+ secretion in the CCD, which could be life threatening in a setting of metabolic acidosis. In contrast, mice deficient in neuronal (n)NOS develop metabolic acidosis (41). In rats inhibition of NO by administration of L-NAME impairs urinary acid excretion after acute NH_4Cl loading (35). CCDs taken from such treated rats showed that net bicarbonate absorption was reduced by 40%. These studies strongly suggest that NO is involved in the maintenance of acid-base homeostasis in the distal nephron; however, it has not been established whether NO regulates proton and/or bicarbonate flux by intercalated cells.

Address for reprint requests and other correspondence: G. J. Schwartz, Pediatric Nephrology, Box 777, Univ. of Rochester Medical Center, 601 Elmwood Ave., Rochester, NY 14642 (e-mail: George_Schwartz@urmc.rochester.edu).

The costs of publication of this article were defrayed in part by the payment of page charges. The article must therefore be hereby marked "*advertisement*" in accordance with 18 U.S.C. Section 1734 solely to indicate this fact.

In this study, we examine whether the changes in H^+/HCO_3^- secretion fluxes induced by acidosis are regulated by ET receptor signaling via the NO-guanylate cyclase pathway. We made use of in vitro acid incubation of CCDs that recapitulates the findings of 3 days of in vivo acid loading (21). CCDs taken from normal rabbits secrete net HCO_3^-, and this net flux is made up of a small H^+ secretory flux that is outstripped by a much larger HCO_3^- secretory flux (26, 33). The adaptation to acidosis is associated with both a modest increase in H^+ secretory flux and a large decrease in HCO_3^- secretory flux, with the resultant sum of fluxes being the secretion of net protons (26, 33); that is, a reversal in polarity of net HCO_3^- transport.

METHODS

Animals. Female New Zealand white rabbits (n = 49) weighing 1.6–2.5 (mean 2.04) kg were maintained on standard laboratory chow (Japan Clea) with free access to water (33). Animals were killed by intracardiac injection of 130 mg pentobarbital sodium after premedication with ketamine (44 mg/kg) and xylazine (5 mg/kg). Urine was obtained postmortem by bladder tap; urine pH averaged 7.96 ± 0.02 (SE, n = 49).

Microperfusion of CCDs. CCDs were microdissected and microperfused as performed in this laboratory (26, 33). The average tubule length was 0.9 ± 0.1 mm. Equilibration and transport were performed using Burg's solution in the perfusate and bath, containing (in mM) 120 NaCl, 25 $NaHCO_3$, 2.5 K_2HPO_4, 2 $CaCl_2$, 1.2 $MgSO_4$, 5.5 D-glucose, 1 trisodium citrate, 4 sodium lactate, and 6 L-alanine, 290 ± 2 mosmol/kgH_2O, and gassed with 94% O_2-6% CO_2, yielding a pH of 7.4 at 37°C (26, 33, 34). Bath was continually exchanged at 14 ml/h by a peristaltic pump. Luminal perfusion rate was maintained at 1.5–2.1 nl/min.

Incubation for 3 h at low pH (pH 6.8 in both luminal and bathing solutions) has been previously described (21). Briefly, the luminal solution contained DMEM without $NaHCO_3$ (GIBCO, BRL, Gaithersburg, MD), Burg's solution, and dissection solution (Burg's solution with 25 mM $NaHCO_3$ replaced by NaCl) in a ratio of 3:2:4, respectively. The bathing solution was similar except that it also contained 30 U/ml penicillin, 30 μg/ml streptomycin, and 3.3% fetal calf serum (GIBCO, BRL) (21, 33, 46). Incubation at pH 6.8 in vitro yields a physiology comparable to 3 days of acidosis in vivo and reverses the polarity of HCO_3^- flux from net secretion to net absorption (21, 26, 33).

Bicarbonate transport. Triplicate collections of 12–15 nl of tubular fluid were made under water saturated mineral oil and analyzed for HCO_3^- using a Nanoflo (WPI, Sarasota, FL) (26, 33, 35, 36). Net HCO_3^- was calculated as $J_{HCO3} = (C_O - C_L) \times (V_L/L)$, where C_O and C_L are the HCO_3^- concentrations of perfused and collected fluid, respectively, V_L is the rate of collected fluid, and L is the length of the tubule (mm) (26, 33). When HCO_3^- transport (J_{HCO3}) is >0, there is net HCO_3^- absorption; when J_{HCO3} is <0, there is net HCO_3^- secretion. To distinguish between unidirectional H^+ and HCO_3^- secretion after net HCO_3^- transport is measured, luminal Cl^- was replaced by gluconate (21). In this maneuver, HCO_3^- is not secreted, thereby uncovering the unidirectional H^+ secretory flux. Subtracting this H^+ secretory flux from the net bicarbonate transport flux reveals the HCO_3^- secretory flux.

Measurements were repeated after the 3-h incubation and compared with preincubation values. In most of the experiments, an agent was introduced in the bath for 30 min at pH 7.4 before being added to the pH 6.8 bathing solution for the 3-h incubation (21, 26). The agents included BQ-788 (1 μM, Sigma, ET_B receptor antagonist) (8), BQ-123 (1–10 μM, Sigma, ET_A receptor antagonist) (2), L-NAME (1 mM, Sigma, St. Louis, MO and Tokyo, Japan, NOS inhibitor) (39), D-NAME (1 mM, Sigma, inactive enantiomer control), LY-83583 (or 6-anilino-5,8-quinolinedione, 10 μM, Biomol, Plymouth Meeting, PA, guanylate cyclase inhibitor) (39), and KT-5823 (2 μM, Sigma, specific cell-permeant cGMP-dependent protein kinase inhibitor) (16).

Transepithelial voltage (mV) was measured using the luminal perfusion pipette as an electrode. The voltage difference between calomel cells connected via 3 M KCl agar bridges to perfusate and bath was measured with a high-impedance electrometer.

Cell pH studies. Cell pH was measured by excitation ratio fluorometry (490 nm/445-nm excitation; 520-nm emission) using 5–10 μM BCECF (Molecular Probes, Eugene, OR) (26, 36). Fluorescence was detected in multiple intercalated cells and corrected for background (Photon Technology, London, Ontario). Movement and contaminating fluorescent signals were minimized by examining cells in focus close to the perfusion pipette and in the wall of the tubule. Duplicate readings were averaged in Burg's solution, after the reversible removal of luminal Cl^- and subsequently after the reversible removal of basolateral Cl^-. The sequence of readings was repeated in the same identified intercalated cells after 3-h incubation.

Agents were dissolved in 0.1% DMSO (vehicle) and added to the bathing solution 3–15 min before and during the 3-h incubation at pH 6.8. These agents included BQ-788 (1 μM, the ET_B receptor antagonist) and L-NAME (1 mM).

Statistics. Data are presented as means ± SE. Standard paired and unpaired comparisons were performed on spreadsheets using Excel 2003 (Microsoft, Bellvue, WA). One-way ANOVA, box plots, and post hoc Duncan and Scheffé's multiple comparison tests were used to examine the acid-incubated/basal H^+/HCO_3^- flux ratios and the acid-induced changes in net HCO_3^- flux using NCSS 6.0 statistical software (Kaysville, UT). Significance was asserted if $P < 0.05$ for each multiple comparison test.

RESULTS

Incubation at pH 6.8 induces a reversal in polarity of net HCO_3^- flux. To study the adaptation of intercalated cells, we utilized the model of in vitro acid incubation (21) and examined the effect of 3-h incubation of each CCD at pH 6.8 in both luminal and bathing solutions. In three CCDs taken from normal rabbits, the mean rate of bicarbonate transport before acid incubation was −3.18 ± 0.51 pmol·min^{-1}·mm^{-1}, indicating net HCO_3^- secretion. After 3-h incubation at pH 6.8, the solutions were restored to pH 7.4 and HCO_3^- transport was remeasured in the same tubule. After acid incubation the net flux was +3.07 ± 0.28 pmol·min^{-1}·mm^{-1} ($P < 0.05$), indicating net H^+ secretion, as has been shown previously (21). The transepithelial voltage became less negative after acid incubation, in keeping with a higher rate of net H^+ secretion (−2.9 ± 0.1 to −2.4 ± 0.1 mV, $P < 0.05$).

To dissect out the unidirectional fluxes of HCO_3^- and H^+ comprising the net flux, we incubated five CCDs at pH 6.8 and added a period in which luminal Cl^- was removed (and replaced by gluconate) to the pre- and postacid-incubation measurements. Bicarbonate transport in the absence of luminal Cl^- reflects the secretion of protons by α-intercalated cells, because HCO_3^- secretion is simultaneously inhibited in the β-intercalated cells. Figure 1 shows that the mean rate of net HCO_3^- transport was −3.81 ± 0.21 pmol·min^{-1}·mm^{-1}, which was comprised of an H^+ secretion rate of 3.69 ± 0.16 pmol·min^{-1}·mm^{-1} and a HCO_3^- secretion rate of −7.50 ± 0.36 pmol·min^{-1}·mm^{-1} (Table 1). After 3-h incubation at pH 6.8 in the presence of vehicle, the net HCO_3^- flux reversed polarity to net H^+ secretion (+3.27 ± 0.14 pmol·min^{-1}·mm^{-1}, $P < 0.01$); at 7.1 pmol·min^{-1}·mm^{-1} (Fig. 2), the change in net flux from basal to acid incubated was large enough to result in a change in

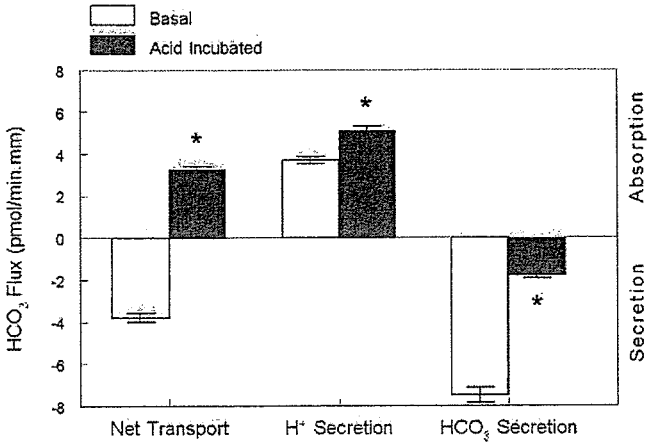

Fig. 1. Changes in H^+/HCO_3^- flux induced by incubation of cortical collecting duct (CCD) at pH 6.8 (n = 5 CCDs). *Left*: net bicarbonate transport. *Middle*: H^+ secretory fluxes obtained from luminal Cl^- removal (which inhibits HCO_3^- secretion). *Right*: HCO_3^- secretory fluxes obtained from the difference between the net and H^+ secretion flux. Each flux is presented before and following acid incubation. *Significantly different ($P < 0.01$) from basal value.

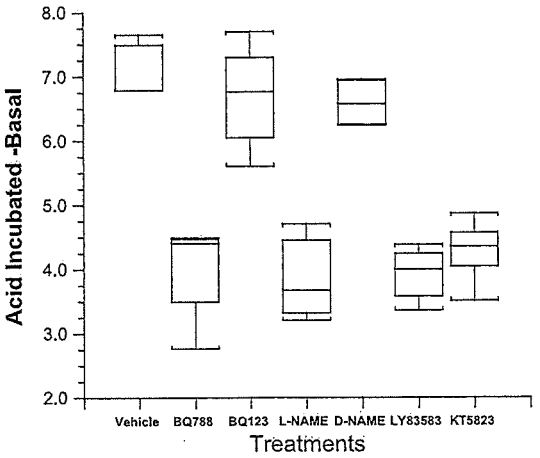

Fig. 2. Inhibition of ET_B receptor signaling blocks adaptive changes in net bicarbonate flux induced by acid incubation. The difference between acid-incubated and basal net bicarbonate flux in pmol·min^{-1}·mm^{-1} under various treatments is shown in box plots. Treatments include vehicle (n = 5), BQ-788 (n = 5), BQ-123 (n = 5), L-NAME (n = 4), D-NAME (n = 4), LY-83583 (n = 6), and KT-5823 (n = 6). The horizontal line represents the median, the *top* and *bottom* of the box represent the 75th and 25th percentiles, respectively, and the length of the box is the interquartile range; the T-shaped lines represent upper and lower adjacent values, wherein the former is the largest observation that is less than or equal to the 75th percentile plus 1.5 times the interquartile range and the latter is the smallest observation that is greater than or equal to the 25th percentile minus 1.5 times the interquartile range. The change in net bicarbonate flux is positive, indicating a shift from net secretion to zero net flux or to net HCO_3^- absorption. Because 1-way ANOVA was highly significant ($P < 0.001$), Duncan and Scheffé's multiple-comparison tests were performed. The change in vehicle net flux was significantly different from those due to BQ-788, L-NAME, LY-83583, and KT-5823, and the changes due to the inactive agents D-NAME and BQ-123 were also significantly different from these 4 treatments. The changes due to BQ-788, L-NAME, LY-83583, and KT-5823 were each significantly different from those due to vehicle, BQ-123, or D-NAME.

polarity from net HCO_3^- secretion to absorption. This adaptation was associated with a 39% increase in H^+ secretory flux to 5.08 ± 0.23 pmol·min^{-1}·mm^{-1} ($P < 0.05$; Table 1 and Fig. 3) and a 76% decrease in HCO_3^- secretory flux to −1.81 ± 0.11 pmol·min^{-1}·mm^{-1} ($P < 0.01$); the acid-incubated flux was 24% of the basal flux (Table 1 and Fig. 4). Concomitant with the increase in H^+ secretion, the transepithelial voltage tended to become less negative after acid incubation (−2.5 ± 0.1 to −2.1 ± 0.2 mV, $P = 0.06$).

Adaptive changes in H^+/HCO_3^- secretion fluxes induced by low pH are inhibited by ET_B receptor antagonism. Because ET secretion is induced by acidosis (42, 44) and ET receptor signaling regulates ion transport processes along the nephron (13, 32, 43), we examined the effect of ET receptor antagonism on the changes in H^+/HCO_3^- secretory fluxes induced by incubation at low pH. Acid incubation with BQ-788 failed to reverse the polarity of the net HCO_3^- flux (Table 1); that is, net HCO_3^- secretion was reduced to no significant HCO_3^- transport (−4.03 ± 0.29 to 0.047 ± 0.16 pmol·min^{-1}·mm^{-1}, $P <$ 0.01); at 4.1 pmol·min^{-1}·mm^{-1}, the change in net flux was significantly smaller than vehicle (Fig. 2). The reduction in net HCO_3^- secretion was not due to an offsetting increase in H^+ secretion [3.95 ± 0.10 to 4.05 ± 0.20, P = not significant (NS); Table 1 and Fig. 3, significantly smaller than vehicle], but rather to a 49% reduction in HCO_3^- secretion (−7.98 ± 0.35 to −4.00 ± 0.15 pmol·min^{-1}·mm^{-1}, $P < 0.01$); the acid-incubated HCO_3^- secretory flux was 51% of the basal flux (Table 1 and Fig. 4) and significantly larger than vehicle. The lack of change in H^+ secretion was associated with no significant change in transepithelial voltage (−2.13 ± 0.15 to −2.04 ± 0.14 mV, P = NS). BQ-123, an ET_A receptor

Table 1. *Basal and acid incubation net and H^+/HCO_3^- fluxes*

		Net Flux			H^+ Flux			HCO_3^- Flux		
Treatment	N	Basal	Acid	Δ	Basal	Acid	%	Basal	Acid	%
Vehicle	5	−3.8±0.21	3.3±0.14†	7.1	3.7±0.16	5.1±0.23*	39	−7.5±0.36	−1.8±0.11†	24
BQ-788	5	−4.0±0.29	0.1±0.16†	4.1	3.9±0.10	4.0±0.20	3	−8.0±0.35	−4.0±0.15†	51
BQ-123	5	−4.1±0.15	2.6±0.22†	6.7	3.5±0.18	4.9±0.22†	42	−7.6±0.26	−2.3±0.31†	30
L-NAME	4	−3.7±0.37	0.2±0.19†	3.8	3.2±0.06	3.9±0.08†	24	−6.8±0.38	−3.8±0.12†	56
D-NAME	4	−3.8±0.07	2.8±0.18†	6.6	3.6±0.19	4.9±0.22†	37	−7.4±0.22	−2.2±0.12†	29
LY-83583	6	−3.8±0.17	0.2±0.09†	3.9	3.2±0.11	3.8±0.18*	16	−7.0±0.27	−3.6±0.23†	51
KT-5823	6	−4.2±0.15	0.1±0.05†	4.3	3.6±0.12	4.0±0.12*	11	−7.9±0.22	−3.9±0.13†	50

Values are means ± SE. Fluxes are reported as pmol·min^{-1}·mm^{-1} tubule length; the fluxes have been rounded to 2 significant numbers to facilitate comparisons across the table. Δ Denotes change from basal to acid incubated, % denotes the ratio of acid-incubated/basal unidirectional H^+/HCO_3^- fluxes ×100. Concentrations of drug treatments were as follows: 1μM BQ-788 and 1–10μM BQ-123, D-NAME, 1 mM N^G-nitro-L-arginine methyl ester (L-NAME), 10 μM LY-83583, and 2 μM KT-5823. *Acid incubated significantly different from basal, $P < 0.05$. †Acid incubated significantly different from basal, $P < 0.01$.

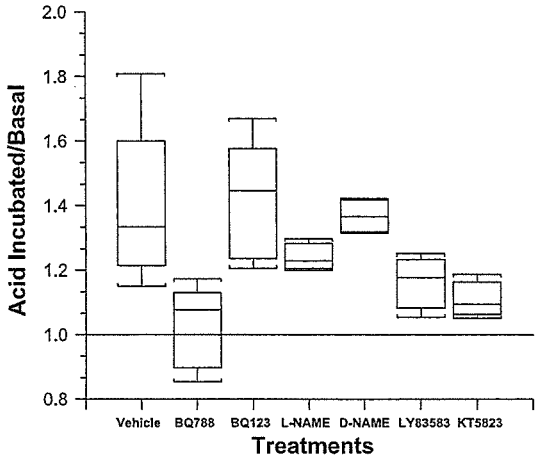

Fig. 3. Antagonism of ET_B receptor blocks increases in H^+ secretion induced by low pH. The ratio of acid-incubated/basal H^+ secretory fluxes under the various treatments is shown. The median and 75th and 25th percentiles are presented as in Fig. 2. The dashed horizontal line denotes the ratio of one, indicating no significant increase in H^+ secretion. ANOVA was highly significant ($P < 0.001$) and the multiple range comparisons showed that the vehicle was significantly different from BQ-788, LY-83583, and KT-5823. The H^+ secretory flux after BQ-788 treatment was significantly different from vehicle, L-NAME, D-NAME, and BQ-123; the BQ-788 ratio includes one within the interquartile range, indicating no significant increase in H^+ secretion with acid incubation. LY-83583 and KT-5823 treatments were significantly different from vehicle, D-NAME, and BQ-123.

antagonist used at 1–10 μM, did not prevent the changes in H^+ secretion and HCO_3^- secretion resulting from the incubation at pH 6.8. Acid incubation with BQ-123 resulted in a reversal of polarity of net HCO_3^- flux that was comparable to CCDs treated with vehicle control (Table 1 and Figs. 2–4). Because the response to acid incubation in the presence of BQ-788 resulted in a larger HCO_3^- secretory flux ($P < 0.05$) and a smaller H^+ secretory flux ($P < 0.05$) than in the presence of vehicle or BQ-123 incubation (Table 1 and Figs. 3 and 4), we concluded that ET_B, but not ET_A, receptor signaling was critical for the adaptation of the CCD to acidosis.

Time control. To ensure the stability of the isolated CCD preparation, we performed four timed control experiments with a 3-h incubation at pH 7.4; three of these experiments utilized 1 μM BQ-788 and the fourth used no inhibitor. Net bicarbonate secretion was unchanged by the incubation (or inhibitor): -3.89 ± 0.16 before and -3.83 ± 0.17 pmol·min^{-1}·mm^{-1} after incubation (P = NS). There was no change in H^+ secretory flux (3.44 ± 0.05 to 3.68 ± 0.21 pmol·min^{-1}·mm^{-1}, P = NS) or in HCO_3^- secretory flux (-7.33 ± 0.13 to -7.51 ± 0.29 pmol·min^{-1}·mm^{-1}, P = NS). In agreement with the stability of the H^+ secretory flux, there was no change in transepithelial voltage (-2.1 ± 0.1 to -2.1 ± 0.1 mV, P = NS). Similar data have been reported previously (33).

Adaptive decrease in HCO_3^- secretion flux induced by low pH requires NO synthesis. ET receptor signaling induces activation of NOS activity (9, 10). Therefore, we examined whether NO production was required for adaptation of the CCD to low pH. To detect the effect of NOS inhibition, we incubated five CCDs in 1 μM L-NAME just before and during the pH 6.8 incubation. Net HCO_3^- secretion before the acid incubation averaged -3.22 ± 0.22 pmol·min^{-1}·mm^{-1} and after acid incubation was only slightly greater than zero, 0.59 ± 0.02 pmol·min^{-1}·mm^{-1}. Whereas the change in net HCO_3^- flux was significant ($P < 0.01$), the acid-induced reversal of polarity of HCO_3^- flux was inhibited by L-NAME. When the inactive D-NAME was employed in two CCDs, the full adaptation and reversal of polarity of the net HCO_3^- flux were apparent (preincubation: -2.59 and -3.74 pmol·min^{-1}·mm^{-1}; postacid incubation: 2.94 and 2.79 pmol·min^{-1}·mm^{-1}, respectively).

We further examined the effect of NOS inhibition on the adaptation to low pH (in vitro acidosis) by measuring HCO_3^- transport in the presence and absence of luminal Cl^-. Table 1 shows that acid incubation with L-NAME resulted in a significant reduction, but not a reversal in polarity, of net HCO_3^- transport (-3.66 ± 0.37 to 0.16 ± 0.19 pmol·min^{-1}·mm^{-1}, $P < 0.01$); at 3.8 pmol·min^{-1}·mm^{-1}, the change in net flux was significantly smaller than vehicle (Fig. 2). This attenuated adaptation was associated with a 24% increase in H^+ secretory flux (3.17 ± 0.06 to 3.93 ± 0.08 pmol·min^{-1}·mm^{-1}, $P < 0.01$; Fig. 3) and a 44% decrease in HCO_3^- secretory flux (-6.84 ± 0.38 to -3.77 ± 0.12 pmol·min^{-1}·mm^{-1}, $P < 0.01$; Fig. 4); at 56%, the ratio of acid-incubated basal HCO_3^- secretory flux was significantly increased over vehicle, indicating a failure to adaptively reduce HCO_3^- secretion during acid incubation. The small increase in H^+ secretion was not associated with a significant decrease in transepithelial voltage (-2.3 ± 0.1 to -2.1 ± 0.2 mV, P = NS). In contrast, for CCDs incubated at pH 6.8 with the inactive enantiomer D-NAME, there was a complete adaptive reversal of polarity of net HCO_3^- flux (Table 1 and Figs. 2–4), similar to what was observed with vehicle control. These data show that NOS inhibition via L-NAME diminishes the downregulation of HCO_3^- secretion that occurs in response to incubation at low pH. L-NAME also partially blocks the acid-induced increase in H^+ secretion (24 vs. 37% for D-NAME; Table 1) but was not

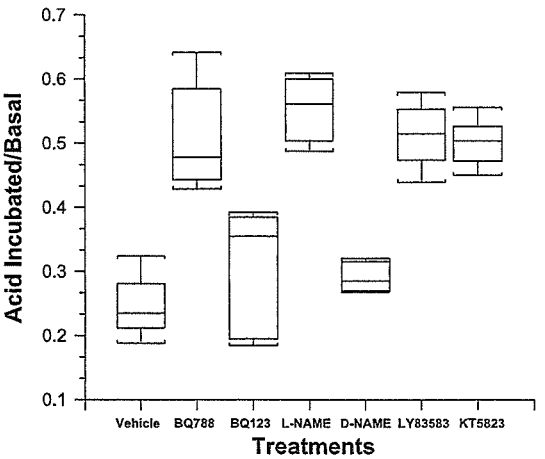

Fig. 4. Inhibition of ET_B receptor signaling blocks adaptive changes in HCO_3^- secretion induced by acid incubation. The ratio of acid-incubated/basal HCO_3^- secretory fluxes under the various treatments is shown. The median and 75th and 25th percentiles are presented as in Fig. 2. ANOVA was highly significant ($P < 0.001$) and the multiple range comparisons showed that vehicle was significantly different from BQ-788, L-NAME, LY-83583, and KT-5823 but was not different from D-NAME or BQ-123. D-NAME and BQ-123 were significantly different from BQ-788, L-NAME, LY-83583, and KT-5823. Each of the active treatments (BQ-788, L-NAME, LY-83583, and KT-5823) was significantly different from vehicle, BQ-123, and D-NAME.

as effective as the ET_B receptor antagonist, BQ-788 (Table 1 and Fig. 2), so that the end result is not a reversal in polarity of HCO_3^- transport, but a reduction to zero net transport.

ET_B receptor antagonism and L-NAME block the effect of acidosis on chloride-dependent cell pH changes. To confirm the changes in HCO_3^- transport, we examined β-intercalated cell pH changes in response to removal of Cl^- from the lumen or bath. Previously, we showed that β-intercalated cells express apical Cl^-/HCO_3^- exchangers and basolateral Cl^- conductances (21, 25). Figure 5*A* shows that when luminal Cl^- was removed, intercalated cell pH rose by 0.40 ± 0.04 pH U, but that after acid incubation, there was no alkalinization of cell pH with this maneuver (delta pH = −0.01 ± 0.03, $P <$ 0.01). When bath Cl^- was removed before the incubation, intercalated cell pH fell by −0.42 ± 0.01 pH U (Fig. 5*B*), but after acid incubation, the change in pH was reduced (delta pH = −0.18 ± 0.05, $P < 0.05$). Such an adaptation to reduce apical Cl^-/HCO_3^- exchange and basolateral Cl^- exit would be appropriate during metabolic acidosis.

BQ-788 added to the pH 6.8 incubation prevented the adaptive reduction in apical Cl^-/HCO_3^- exchange (0.46 ± 0.02 to 0.46 ± 0.01 pH U, P = NS; Fig. 5*C*) and in sensitivity to basolateral Cl^- removal (−0.44 ± 0.03 to −0.44 ± 0.04, P = NS; Fig. 5*D*). Similarly, L-NAME added to the pH 6.8 incubation clearly prevented the reduction in apical Cl^-/HCO_3^- exchange (0.47 ± 0.03 to 0.45 ± 0.03 pH U, P = NS; Fig. 5*E*) and in sensitivity to basolateral Cl^- removal (−0.48 ± 0.04 to −0.51 ± 0.05 pH U, P = NS; Fig. 5*F*). These results confirm that ET_B receptor signaling and NO synthesis are required for the adaptive decrease in HCO_3^- secretion (presumably by endocytosis of apical Cl^-/HCO_3^- exchangers) induced by incubation at low pH.

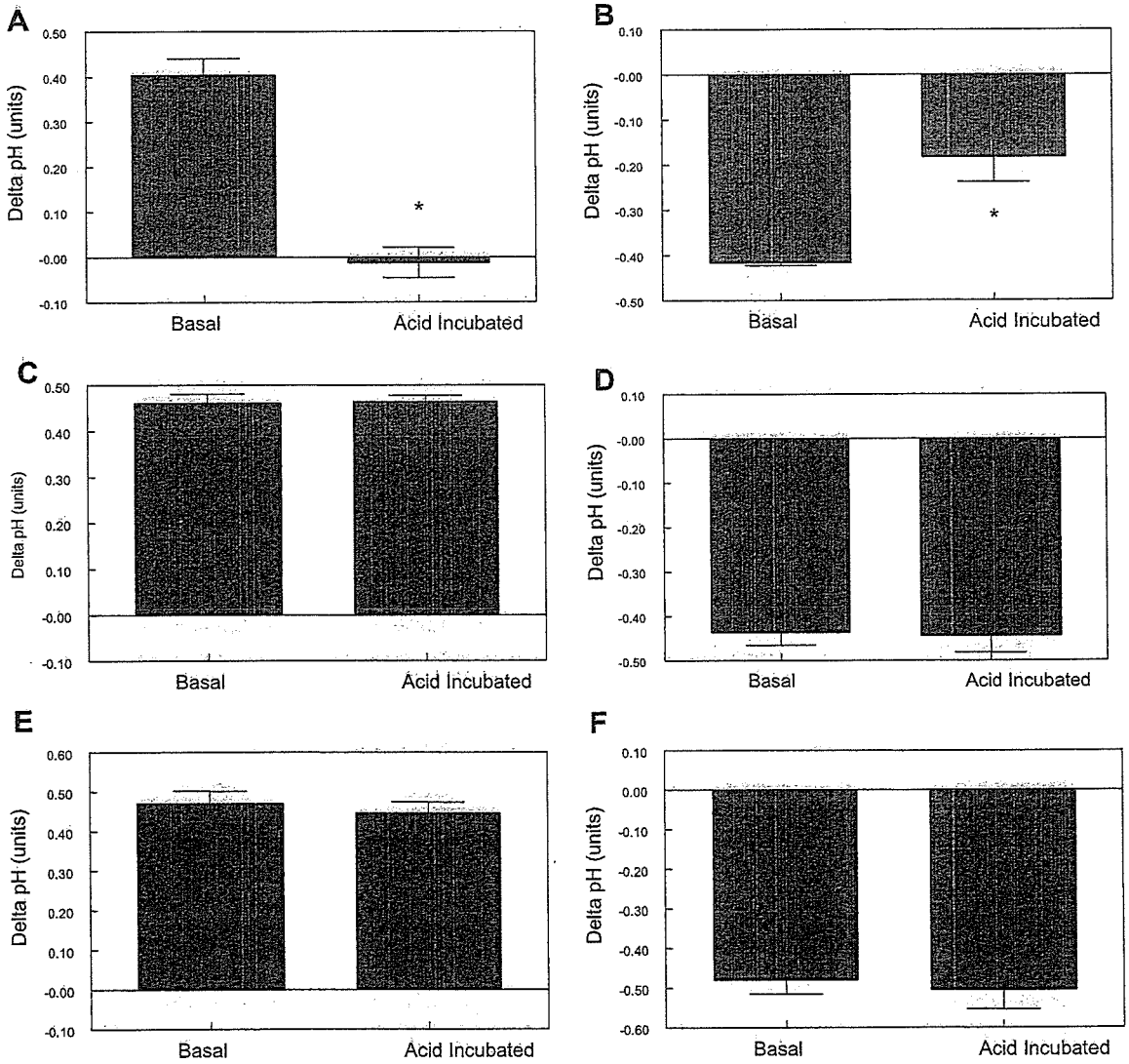

Fig. 5. ET_B receptor signaling is required for loss of luminal Cl^-/HCO_3^- exchange activity stimulated by low pH. Cell pH changes in response to Cl^- removal in basal state and after acid incubation are shown. *A*, *C*, and *E*: intercalated cell pH changes resulting from luminal Cl^- removal. *B*, *D*, and *F*: cell pH changes resulting from bath Cl^- removal. *A* and *B*: vehicle (n = 25 cells from 3 CCDs). *C* and *D*: BQ-788 (n = 40 cells from 5 CCDs). *E* and *F*: L-NAME (n = 66 cells from 7 CCDs). *Significantly different from basal value ($P < 0.01$).